Design and Synthesis of Novel Derivatives of the Muscarinic Agonist Tetra(ethylene glycol)(3-methoxy-1,2,5-thiadiazol-4-yl) [3-(1-Methyl-1,2,5,6-tetrahydropyrid-3-yl)-1,2,5-thiadiazol-4-yl] Ether (CDD-0304): Effects of Structural Modifications on the Binding and Activity at Muscarinic Receptor Subtypes and Chimeras

Frederick R. Tejada, Peter I. Nagy, Min Xu, Cindy Wu, Tricia Katz, Jason Dorsey, Melissa Rieman, Elizabeth Lawlor, Manya Warrier, and William S. Messer, Jr.*

Departments of Medicinal & Biological Chemistry and Pharmacology, The University of Toledo, 2801 W. Bancroft St., Toledo, Ohio 43606

Received June 9, 2006

As part of a continuing effort to design and synthesize highly selective muscarinic agonists for different muscarinic receptor subtypes, several tetra(ethylene glycol)(3-methoxy-1,2,5-thiadiazol-4-yl) [3-(1-methyl-1,2,5,6-tetrahydropyrid-3-yl)-1,2,5-thiadiazol-4-yl] ether (**1**) analogues were prepared and characterized. Different analogues were synthesized having hydrophilic spacers of di-, tri-, tetra-, penta(ethylene glycol) and tri(propylene glycol) separating the 1,2,5,6-tetrahydropyridine ring from the terminal heterocycle, which was either a 1,2,5-thiadiazole or 1,2,4-thiadiazole ring. Chimeric receptor and molecular modeling studies also were conducted to determine how the ligands interact with muscarinic receptors. The studies revealed that varying the distance of the terminal thiadiazole and the positioning of the methoxy group can increase binding affinity for certain muscarinic receptor subtypes (at M_2 for **13d** and M_4 for **1**) and enhance functional efficacy at M_4 receptors for **13e** and **18b**. Moreover, compound **1** exhibited antipsychotic activity as assessed by reversal of apomorphine-induced sensory motor gating deficits, suggesting potential utility in the treatment of schizophrenia.

Introduction

Schizophrenia, a psychiatric disorder, afflicts approximately 2 million Americans. The strategies for developing antipsychotics have been significantly influenced by the dopamine hypothesis of schizophrenia.[1] However, even the new atypical antipsychotics do not completely relieve all schizophrenic symptoms.[2] In particular, these agents are relatively ineffective against cognitive deficits associated with schizophrenia. It has been shown that schizophrenic patients suffer from impairments of mnemonic function affecting both verbal and episodic long-term memory and language use. These cognitive deficits may be due to the observed alterations found in the brains of schizophrenic patients, i.e., reduced numbers of muscarinic and nicotinic receptors in the cortex and hippocampus.[3]

Cognitive deficits, including impaired working memory, attention, and executive functions, are strongly linked to the long-term disabilities found in patients with schizophrenia.[4] Despite this, relatively few efforts have focused on developing compounds that can improve cognitive disturbances associated with schizophrenia.[5] The cognitive deficits associated with schizophrenia represent an important clinical target for drug development that has not been addressed by the pharmaceutical industry.

Several lines of evidence suggest that selective muscarinic agonists might be useful in the treatment of schizophrenia. Muscarinic agonists including xanomeline (Figure 1A) have been shown to be active in animal models with similar profiles to known antipsychotic drugs.[6] In a small clinical trial, xanomeline reduced the positive, negative, and cognitive symptoms in treatment-resistant schizophrenic patients.[7] Further, the selective M_1 and M_4 agonist xanomeline was shown to significantly improve psychiatric symptoms in phase II clinical trials in Alzheimer's patients.[8] Unfortunately, xanomeline produced unwanted side effects associated with the activation

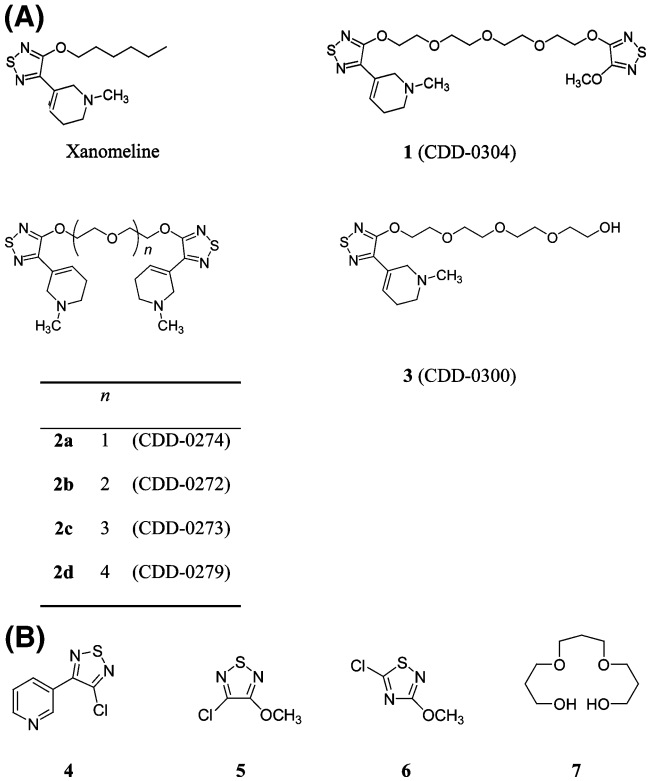

Figure 1. (A) Structures of the 1,2,5,6-tetrahydropyridine compounds and (B) structures of key starting materials.

* To whom correspondence should be addressed. Phone: 419-530-1958. Fax: 419-530-1909. E-mail: wmesser@utoledo.edu.

10.1021/jm0606995 CCC: $33.50
Published on Web 11/14/2006

of M_3 receptors that severely limit the clinical utility of this compound.[9] Follow-up preclinical studies with structurally related compounds identified strong antipsychotic activity in (5*R*,6*R*)-6-(3-butylthio-1,2,5-thiadiazol-4-yl)-1-azabicyclo[3.2.1]-octane (BuTAC), which displays partial agonist activity at M_2 and M_4 receptors.[10] Muscarinic agonists such as xanomeline and BuTAC may exert an antipsychotic action by regulating the release of dopamine in the frontal cortex.[11−13] Xanomeline and BuTAC produce very few of the adverse side effects (e.g., catalepsy) associated with classical antipsychotics such as haloperidol, suggesting that selective muscarinic agonists might provide a useful alternative therapeutic approach to treating the symptoms of schizophrenia. Moreover, muscarinic agonists might be useful in improving cognitive function (including memory function, language use, and constructional praxis) in schizophrenic patients.[5]

Of the five known muscarinic receptors, M_1 receptors are found in high abundance within the cerebral cortex and hippocampus brain regions implicated in memory and cognitive function.[14] Post-mortem and genetic study suggest that activating the M_1 receptor might be critical in reversing the cognitive deficits in schizophrenia.[15] Similar to M_1 receptors, M_2 receptors also are expressed in the hippocampus and most other brain regions implicated in learning and memory processes. Since M_1 and M_2 receptors play a role in cognitive and memory function,[16−18] agonists with M_1 and M_2 activity might be particularly useful in treating memory and cognitive deficits associated with schizophrenia.[5,13] On the other hand, M_4 receptors regulate the release of dopamine and have been implicated in schizophrenia.[13,19] A recent study indicates that loss of midbrain M_4 receptors in knockout mice causes a state of dopaminergic hyperexcitability.[20] This in turn may be responsible for the pathological mechanism for affective and cognitive disorders and psychoses, in which dysregulated dopaminergic transmission plays a key role. Taken together, an M_1, M_2, and M_4 agonist could provide efficacy in a broad range of symptomatic domains of schizophrenia, including enhancement of cognitive function.

Several model systems have been developed for assessing the antipsychotic activity of novel compounds. Compounds such as apomorphine and phencyclidine alter normal rodent responses in the prepulse inhibition (PPI) of startle response and conditioned avoidance paradigms. The PPI response assesses sensorymotor gating in rodents, whereby a tone immediately preceding a loud stimulus results in a diminished startle response. The PPI paradigm is particularly attractive, since it assesses the integrity of a normal behavior found in both rodents and humans. Schizophrenia patients display an attenuated PPI response, while apomorphine also attenuates the PPI response in rodents by altering dopamine activity in the mesolimbic system.[21] Classical and atypical antipsychotics are effective in reversing the effects of apomorphine on the PPI response, and muscarinic agonists such as xanomeline and (5*R*,6*R*)-6-(3-propylthio-1,2,5-thiadiazol-4-yl)-1-azabicyclo[3,2,1]octane (PTAC) also display activity in the PPI paradigm.[22] Behavioral studies addressing cognitive aspects of schizophrenia have focused on working memory function, since working memory appears to be a core deficit that leads to impairment of other cognitive domains.[23,24]

The clinical utility of muscarinic agonists for the treatment of schizophrenia has not been adequately assessed due to the lack of compounds exhibiting an appropriate combination of agonist activity and selectivity for M_1, M_2, and M_4 receptors. Recently, a bivalent derivative of xanomeline, **2c** (Figure 1A), was developed with strong agonist activity at M_1 and M_4 receptors and very low activity at M_3 and M_5 receptors.[25] While bivalent ligands (i.e., **2c**) are unsuitable as drug candidates due to their limited membrane permeability and bioavailability, they have helped define accessory binding sites for muscarinic ligands with improved receptor subtype selectivity. In a continuing effort to design and develop M_1, M_2, and M_4 selective muscarinic agonists, a second-generation derivative containing a terminal thiadiazole moiety was synthesized and pharmacologically evaluated. Tetra(ethylene glycol)(3-methoxy-1,2,5-thiadiazol-4-yl) [3-(1-methyl-1,2,5,6-tetrahydropyrid-3-yl)-1,2,5-thiadiazol-4-yl] ether, **1** (Figure 1A), displayed functional activity at M_1 and M_2 receptors and partial agonist activity at M_4 receptors and was essentially inactive at M_3 and M_5 receptors. Further in vivo studies verified the subtype selectivity and good penetration into the central nervous system for **1**.[26]

Compound **1** thus represents a lead compound for the development of selective muscarinic agonists with potential utility in the treatment of schizophrenia. Preliminary chimeric receptor data suggest that amino acids found in the second and third extracellular loops of the M_1 receptor are critical for agonist binding and activity, respectively. Hence, analogues of **1** with variable hydrophilic spacers and terminal group were designed to investigate the effect on binding and activity at the different muscarinic receptor subtypes. Chimeric receptor studies were conducted to help assess the molecular details of the binding, activity, and selectivity of the novel series of muscarinic agonists. This paper will also assess safety and the potential therapeutic utility of **1** and related compounds in the treatment of schizophrenia and other psychiatric disorders.

Chemistry

The key intermediate 3-(3-chloro-1,2,5-thiadiazol-4-yl)pyridine, **4** (Figure 1B), was synthesized using published procedures.[27] The terminal thiadiazoles 3-chloro-4-methoxy-1,2,5-thiadiazole and 5-chloro-3-methoxy-1,2,4-thiadiazole, **5** and **6**, respectively, were also prepared using published procedures (Figure 1B).[26,28] The various ethylene glycol spacers were commercially available, while the tripropylene glycol spacer, **7**, was prepared from 1,3-propanediol (Figure 1B).[29] The polyglycol spacer was of particular importance, as it could be modified in length and hydrophilicity and the terminus could be easily functionalized. The tripropylene glycol series was made to investigate the effect of a relatively less flexible spacer on binding affinity and functional activity.

The pyridinyl compounds **10** and **15** were prepared by the Williamson ether formation method to incorporate the polyglycol spacers and the corresponding terminal thiadiazoles (Schemes 1 and 2). The monoquaternary compounds **11** and **16** were easily obtained by alkylation of the corresponding pyridine with iodomethane. The compounds were then reduced by sodium borohydride to the corresponding 1,2,5,6-tetrahydropyridyls. Finally, the free bases were converted to the HCl salt using ethereal HCl.

Pharmacology

The binding affinities of the synthesized compounds were evaluated using cloned human mAChR subtypes expressed in A9 L cells according to methods described previously.[26] To determine the functional properties of the various synthesized compounds, two novel methods were successfully developed and validated. The scintillation proximity assay (SPA) was used for measuring M_1, M_3, and M_5 receptor-stimulated phosphoinositide (PI) hydrolysis. This method is based upon selective detection of radiolabeled inositol phosphate in the presence of

Scheme 1. Synthesis of 1,2,5,6-Tetrahydropyridine Compounds with *n*-Ethylene Glycol Spacer[a]

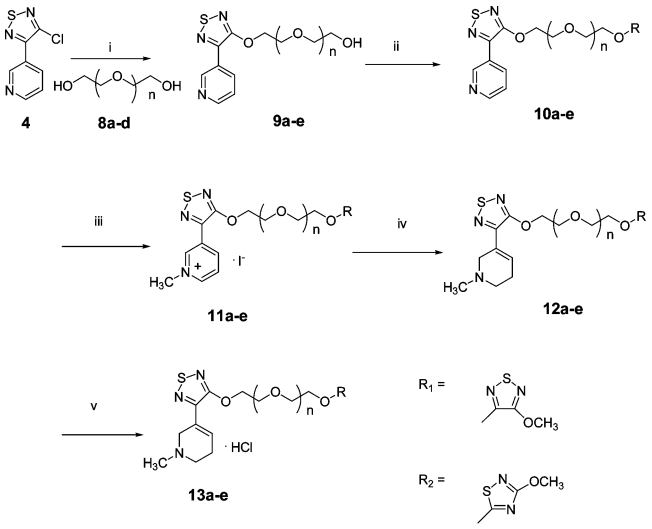

Compound	n	R
13a	1	R_1
13b	2	R_1
1	3	R_1
13d	4	R_1
13e	3	R_2

[a] Reagents: (i) NaH/THF, *n*-ethylene glycol, (ii) NaH/THF, thiadiazole group (**5** or **6**), (iii) iodomethane, acetone, (iv) $NaBH_4$, $MeOH/CHCl_3$, (v) HCl, ether/acetone.

radiolabeled inositol using SPA technology. The basis for the detection is the anion-exchanging property of the SPA beads that alleviates any filtration step. Compared with older methods using anion-exchange cartridges, this method not only simplifies and accelerates PI turnover assays but makes this general assay accessible to high-throughput, automated laboratories. On the other hand, a new method using enzyme fragment complementation technology was used for measuring M_2 and M_4 receptor-stimulated cyclic adenosine monophosphate (cAMP) formulation. This method has the advantages of increased sensitivity for detecting basal levels of cAMP and observing activation of adenylyl cyclase by forskolin. Compared with the direct cAMP enzyme immunoassay used previously, this new method is more direct, faster, less variable, and amenable to high-throughput assays.[30] Carbachol and xanomeline were used as reference compounds. Ligand-binding affinities, expressed as pK_i values, of the synthesized compounds were determined and are shown in Tables 1 and 2. The functional properties of agonists were expressed as pEC_{50} or pIC_{50} values to assess potency and the maximal level of stimulation (S_{max}) or inhibition (I_{max}) for the efficacy of the compounds and are reported in Table 3.

A series of site-directed mutagenesis and chimeric receptor studies was initiated to assess the relative contributions of amino acids within the transmembrane domains and extracellular loops to the high affinity and selectivity of compounds **1** and **2c**. These studies took advantage of the relatively high activity of compounds **1** and **2c** at M_1 receptors as compared with M_5 receptors. Compounds were characterized at wild-type and chimeric muscarinic receptors as described previously.[26,31−33]

Results and Discussion

In general, the new compounds inhibited the binding of [^{3}H]-(*R*)-QNB in a dose-dependent manner with pK_i values ranging from 5.4 to 8.6 as shown in Tables 1 and 2. Among the ligands, **13a** exhibited significantly higher binding affinities at the M_2, M_3, and M_4 receptor subtypes ($p < 0.01$); **13d** displayed significantly higher binding affinities at M_2, M_4, and M_5 receptor subtypes ($p < 0.001$); both **13b** and **13e** exhibited significantly higher binding affinities at the M_2 and M_4 receptor subtypes (**13b**, $p < 0.01$; **13e**, $p < 0.001$). Two-way ANOVA (ligand × receptor) showed a significant ligand and receptor interaction ($p < 0.0001$), indicating that the ligand-associated binding affinity changes were dependent on receptor subtypes. Ligand and receptor, the two factors, also significantly affected the binding affinity value (pK_i) separately ($p < 0.0001$). Statistical comparisons between one-site and two-site models were carried out using an *F*-test with α set at the 0.05 level. All data for new analogues were fit into a one-site model at M_1 receptors and a two-site model at M_2 receptors, respectively.

In addition, the functional agonist activity (i.e., potency and efficacy) of the compounds at M_1, M_3, and M_5 receptors was assessed using SPA-PI assays and is summarized in Table 3. Compounds **13a**,**b** and **18a**,**b** exhibited lower activity at M_1 receptors than both **1** and xanomeline. Compounds **13d** and **13e** showed relatively yet not significantly higher efficacy than the others ($p > 0.05$), with 28% and 31% the activity of carbachol, respectively. All compounds were inactive at M_3 receptors. On the other hand, **13e** showed weak agonist activity at M_5 receptors (*t* test, $\alpha = 0.05$) yielding 1.2% of the activity of carbachol. Taken together, both **13d** and **13e** exhibited significant functional selectivity for M_1 receptor versus M_5 receptors (**13d**, $p < 0.05$; **13e**, $p < 0.01$).

In contrast, structural modification of the lead compound **1** resulted in new analogues with high efficacy yet lower potency for inhibition of forskolin-stimulated cAMP accumulation in CHO cells stably expressing M_2 receptors. **13b** and **13e** exhibited the same level of activity as carbachol, yielding 112% and 101% inhibition of that of carbachol, respectively. At M_4 receptors, both **13e** and **18b** exhibited significantly higher agonist activities than the others with 148% and 126% inhibition of carbachol's activity, respectively. **13a** and **13d** displayed the same level of efficacy as **1**. Compound **18a** was essentially inactive at M_2, M_3, M_4, and M_5 receptors with modest efficacy at the M_1 receptor, while **18b** was inactive at M_2, M_3, and M_5 receptors. Two-way ANOVA (ligand × receptor) analysis showed a significant ligand and receptor interaction ($p < 0.0001$), indicating that the ligand-associated activity changes were dependent on the receptor subtypes. Ligand and receptor, the two factors, also significantly affected the associated functional activity, separately ($p < 0.0001$).

Effect of Spacer Length. The binding affinites of the compounds toward the various muscarinic receptor subtypes are shown in Table 1. With increasing spacer length, the affinity toward the M_1 receptor was found to reach a maximum at tetraethylene glycol ($n = 3$), where *n* is the repeating glycol unit, whose length is about 9−14 Å, depending on the spacer conformation. In this particular series, the same trend was observed for the functional activities (pEC_{50} and S_{max} values) of the compounds at the M_1 receptor (Table 3). On the other hand, binding affinity was found to increase with increasing spacer length toward the M_2 receptor. However, this trend was not reflected in terms of agonist functional activity. At M_4 receptors, **13b** was found to have the highest efficacy and lowest

Scheme 2. Synthesis of 1,2,5,6-Tetrahydropyridine Compounds with Propylene Glycol Spacer[a]

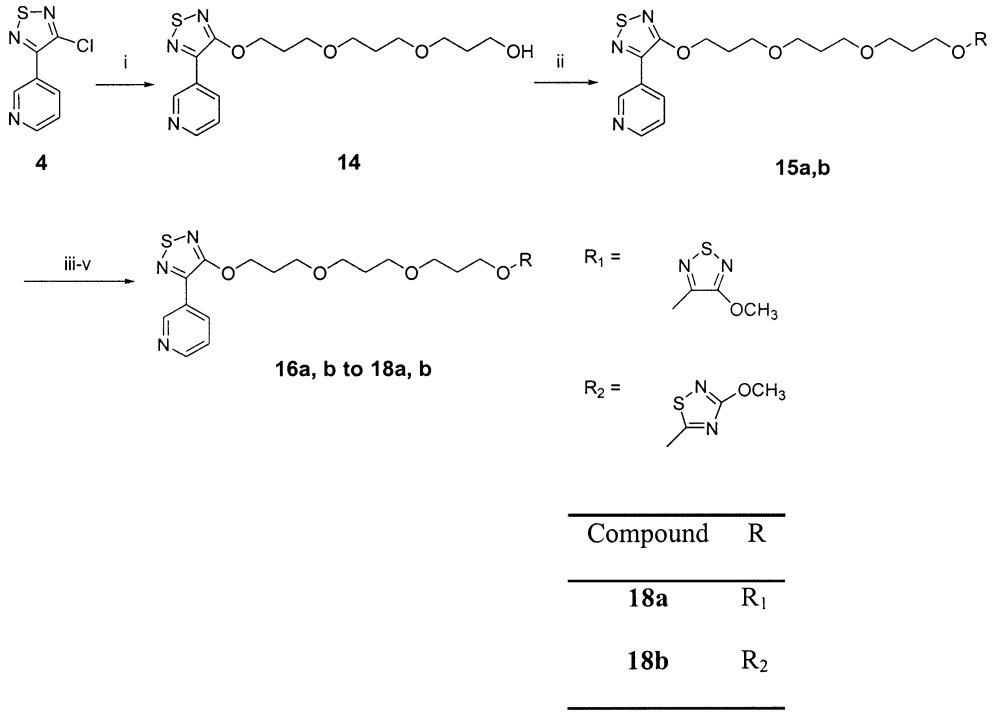

Compound	R
18a	R_1
18b	R_2

[a] Reagents: (i) NaH/THF, tri(propylene glycol) (**7**), (ii) NaH/THF, thiadiazole group (5 or 6), (iii) iodomethane, acetone, (iv) $NaBH_4$, MeOH/$CHCl_3$, (v) HCl, ether/acetone.

Table 1. Effect of Spacer Length on the Inhibition of [^{3}H]-(*R*)-QNB Binding to Human Muscarinic Receptor Subtypes Expressed in A9 Cells[a]

		binding affinities (pK_i ± SEM)				
ligand	n	M_1	M_2	M_3	M_4	M_5
carbachol		5.5 ± 0.1	7.0 ± 0.2	5.2 ± 0.2	6.4 ± 0.3	4.7 ± 0.3
xanomeline		6.8 ± 0.0	7.3 ± 0.2	7.1 ± 0.1	7.4 ± 0.1	5.8 ± 0.1
13a	1	6.1 ± 0.1	7.4 ± 0.2	7.3 ± 0.1	7.2 ± 0.1	6.6 ± 0.2
13b	2	6.5 ± 0.0	7.4 ± 0.1	6.6 ± 0.1	7.1 ± 0.2	6.2 ± 0.0
1	3	7.3 ± 0.3	8.1 ± 0.0	7.6 ± 0.1	8.6 ± 0.1	6.4 ± 0.3
13d	4	6.4 ± 0.0	8.6 ± 0.1	5.8 ± 0.0	7.9 ± 0.2	7.0 ± 0.1

[a] p*K*i values were obtained by nonlinear least-squares curve-fitting of data as described in the Experimental Section. Data represent the mean ± SEM from at least three independent experiments, each performed in triplicate.

Table 2. Effect of Methoxy Positioning and Tri(propylene Glycol) Spacer on Inhibition of [^{3}H]-(*R*)-QNB Binding to Human Muscarinic Receptor Subtypes Expressed in A9 Cells[a]

	binding affinities (pK_i ± SEM)				
ligand	M_1	M_2	M_3	M_4	M_5
carbachol	5.5 ± 0.1	7.0 ± 0.2	5.2 ± 0.2	6.4 ± 0.3	4.7 ± 0.3
xanomeline	6.8 ± 0.0	7.3 ± 0.2	7.1 ± 0.1	7.4 ± 0.1	5.8 ± 0.1
1	7.3 ± 0.3	8.1 ± 0.0	7.6 ± 0.1	8.6 ± 0.1	6.4 ± 0.3
3	6.0 ± 0.1	6.5 ± 0.0	6.5 ± 0.1	6.1 ± 0.0	5.4 ± 0.0
13e	6.7 ± 0.0	7.4 ± 0.1	6.5 ± 0.1	7.6 ± 0.0	6.6 ± 0.0
18a	7.0 ± 0.2	6.8 ± 0.2	6.7 ± 0.1	6.8 ± 0.1	7.0 ± 0.1
18b	7.2 ± 0.0	7.2 ± 0.0	6.7 ± 0.2	6.8 ± 0.2	6.6 ± 0.1

[a] p*K*i values were obtained by nonlinear least-squares curve-fitting of data as described in the Experimental Section. Data represent the mean ± SEM from at least three independent experiments, each performed in triplicate.

potency. This indicates that the optimum distance between the thiadiazole moieties in this series is realized in **1**.

Molecular modeling studies were employed to examine the conformational features that might account for the varying degrees of activity and selectivity within this series of analogues. On the basis of gas-phase calculations, where the new monocations and previously described dications[25] (Figure 1A, **2a**−**d**) were studied in the absence of counterion(s), the electrostatic repulsion of the remote charged sites in dications did not prevent the folding of the spacer. The O_α···O_ω separation along the $-O_\alpha$-$CH_2(CH_2OCH_2)_nCH_2O_\omega-$ moiety in the all-trans conformation increased from 7.3 to 18.2 Å when *n* varied from 1 to 4. The equilibrium gas-phase structures exhibited shorter separations throughout the MD simulations. Part of the reason may be that local gauche conformations emerge also favorably in the equilibration process. Another important factor is the van der Waals interaction of the ring systems. Since the nonbonded cutoff was set to 20 Å, both the electrostatic and van der Waals interactions of the end-group rings were considered. The shorter than maximal O_α···O_ω separations indicate the gauche−trans balance as well as the balance of the repulsive electrostatic and attractive van der Waals forces. The MD simulations in isotonic saline solution models explored the favorable conformational equilibrium for the solute molecules before being affected by interactions with the receptor. Thus, on the basis of such modeling, the structure of the potential ligand molecules could be characterized in the presynaptic cleft. Comparison of the obtained structures with those found for the ligands bound to the receptor helps assess the energy-need for the conformational change required to favorably fit into the transmembrane receptor sites. One of the most important structural parameters in the case of the modeled bivalent molecules is the O_α···O_ω separation. The calculated values are summarized in Figure 2 and Table 4.

As shown in Figure 2, the average O_α···O_ω separation monotonically increases in solution for dications but shows a

Table 3. Stimulation of PI Metabolism through Activation of M_1, M_3, and M_5 Receptors and Inhibition of Adenylyl Cyclase Activity through Activation of M_2 and M_4[a]

		M_1		M_3		M_5		M_2		M_4	
ligand	n	pEC_{50}	S_{max} (%)	pEC_{50}	S_{max} (%)	pEC_{50}	S_{max} (%)	pIC_{50}	I_{max} (%)	pIC_{50}	I_{max} (%)
carbachol		5.3 ± 0.3	100 ± 12	5.3 ± 0.1	100 ± 15	6.0 ± 0.0	100 ± 3.6	7.2 ± 0.1	100 ± 2.9	7.3 ± 0.1	100 ± 3.1
xanomeline		6.5 ± 0.2	71 ± 7.0	4.6 ± 0.3	80 ± 12c	4.9 ± 0.0	43 ± 7.6	nc[b]	na[b]	7.6 ± 0.2[c]	77 ± 12[c]
3	1	6.1 ± 0.2	7.9 ± 1.9	nc	na	nc	7.4 ± 3.6	8.1 ± 0.3	86 ± 9.2	4.6 ± 0.2	110 ± 22
13a	1	6.0 ± 0.2	11 ± 0.8	nc	na	nc	0.83 ± 0.3[e]	7.1 ± 0.1	77 ± 3.4	5.1 ± 0.2	47 ± 6.7
13b	2	6.1 ± 0.1	13 ± 1.5	nc	na	nc	1.3 ± 1.3[e]	5.5 ± 0.2	110 ± 7.5	5.1 ± 0.1	100 ± 10
1[c]	3	7.2 ± 0.1	47 ± 4.4	nc	na	nc	na	9.3 ± 0.3	120 ± 7.4	7.9 ± 0.5	40 ± 11
13d	4	6.6 ± 0.1	28 ± 4.4	nc	na	nc	0.95 ± 0.5[e]	6.4 ± 0.1	98 ± 7.2	6.4 ± 0.3	37 ± 7.5
13e	3	6.6 ± 0.1	31 ± 6.5	nc	na	6.2 ± 0.1	1.2 ± 0.4	6.6 ± 0.0	100 ± 1.6	5.9 ± 0.3	150 ± 18
18a		5.5 ± 0.5	21 ± 2.8	nc	na	nc	0.6 ± 4.2	nc	130 ± 7.7[d]	nc	260 ± 7.8[d]
18b		6.3 ± 0.3	27 ± 13	nc	na	nc	na	nc	na	5.2 ± 0.32	130 ± 18

[a] Maximal responses pEC_{50} and pIC_{50} values were obtained by nonlinear least-squares curve-fitting of data as described in the Experimental Section. Data represent the mean ± SEM from at least three independent experiments, each performed in triplicate. Responses expressed as the percentage of the maximal (or minimal) carbachol response. [b] na, not active; nc, not calculated (due to lack of activity). [c] Data from Cao et al.[26] [d] Inhibition activity at 1 mM. [e] Response at 100 μM.

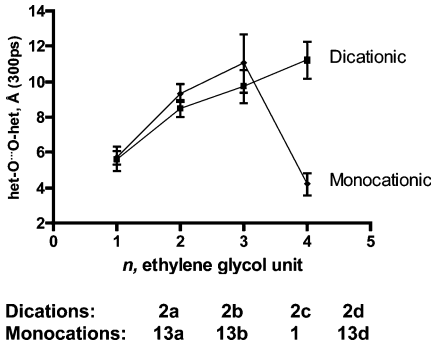

Figure 2. Calculated distance of $O_\alpha \cdots O_\omega$ from molecular dynamic simulations in isotonic saline solution.

maximum as a function of *n* for the monocations. In all cases, the average $O_\alpha \cdots O_\omega$ distance is smaller than the corresponding all-trans separation. Part of the reason was discussed above in relation to the gas-phase MD simulations. A difference is, however, that counterions were also considered in solution; thus, the system was neutral. The counterions (including those from the three $Na^+ \cdots Cl^-$ ion pairs) were found located mainly around the positively charged site(s), providing favorable electrostatic interactions in addition to the electrostatic repulsions for the dications.[25,26] If *n* is large enough, the molecules can take a favorable U-shape structure driven by the attractive van der Waals forces. The effect is most expressed for the monocationic **13d** molecule, where the spacer ($n = 4$) is long and flexible enough to facilitate the stacking position of the thiadiazole rings. As a result, the average $O_\alpha \cdots O_\omega$ distance decreases from 11.1 ± 1.7 to 4.2 ± 0.6 Å when *n* increases from 3 to 4. In order to adopt a remarkably extended conformation, required for the binding in a narrow pore within the receptor, considerable activation energy is expected. The effective spacer length, characterized by the average $O_\alpha \cdots O_\omega$ distance for the free solute in solution, correlates with the binding affinity of the monocationic ligands when the M_1 receptor subtype is considered (Table 1). The trend is similar for the M_4 subtype, and the corresponding pEC_{50} and pIC_{50} values also correlate with the *n* number characterizing the spacer (Tables 1 and 3). These findings suggest that the effective length of the spacer is at least one of the main factors determining the strength of the binding to the M_1 and M_4 subtypes. The correlation with *n* also suggests that in these cases the binding mode is basically an extended conformation, and the binding constant is related both to the effective spacer length and to the activation energy producing the favorable $O_\alpha \cdots O_\omega$ distance. The two effects, too short effective length or too large activation energy for the spacer extension, lead to an optimal combination with largest binding pK_i for M_1 and M_4 subtypes.

Table 4. Optimized $O_\alpha \cdots O_\omega$ Distances for Bound Ligands and the Hydrogen Bonds Formed with the M_1 Wild-Type as well as o3, o2, and o2+o3 Chimeric Receptors[a]

	M_1 WT	o3	o2	o2 + o3
	(A) $O_\alpha \cdots O_\omega$ Distances[b]			
2c	13.5 (13.5)	9.8 (9.7)	13.0 (13.5)	12.2 (12.0)
1	12.8 (11.9)	12.9 (11.8)	10.1 (10.0)	10.5 (13.2)
13e	10.2 (13.1)	12.3 (12.3)	12.3 (12.5)	
	(B) Lengths of H-bonds to the Indicated Residue[b]			
2c	1.62, Glu397 (1.70)	1.67, Asp392 (1.65)	4.34, Glu397 (1.71)	hydrophobic pocket
	1.64, Asp105 (1.72)	1.67, Asp105 (1.66)	1.64, Asp105 (1.76) Lys392/Glu397[c]	1.63, Asp105 (1.87)
1	–	4.28, Lys393 (2.05)	2.98, Lys392 (1.85)	hydrophobic pocket
	1.67, Asp105 (1.65)	1.68, Asp105 (1.66)	1.69, Asp105 (1.65) Lys392/Glu397[c]	5.06, Asp105 (1.68)
13e	–	–	–	
	1.63, Asp105 (1.70)	1.67, Asp105 (1.66)	1.69, Asp105 (1.68) Lys392/Glu397[c]	

[a] Distances in Å. [b] Values in parentheses were obtained from energy minimizations taken after considering all together 200-ps MD simulations. [c] Salt bridge.

Effect of the Terminal Thiadiazole. We reasoned that the ligands in the series of varying spacer length undergo $O_\alpha \cdots O_\omega$ stretching in order to adopt a structure favorable for the binding to the receptor wherein the common protonated tetrahydropyridine site is stably buried in the hypothesized acetylcholine binding site while the other end of the ligands can freely librate and interact with amino acid residues in the loop area. Preliminary chimeric receptor data suggest that amino acids found in the second and third extracellular loops of the M_1 receptor are critical for agonist binding and activity, respectively.

Considering the optimum spacer length in **1**, it was further subjected to modification at the terminal thiadiazole moiety. On the basis of the hypothesis above, the importance of the methoxy moiety was evaluated by replacing the 4-methoxy into a 3-methoxy position and an analogue without the terminal thiadiazoles. The substitution of the terminal 1,2,5-thiadiazole in **1** with 1,2,4-thiadiazole in **13e** resulted in a relative decrease in the binding affinity across the M_1 to M_4 receptors but maintained comparable M_5 binding affinity (Table 2). Although a decrease in M_1 binding affinity was observed, the functional

Table 5. M_3 Receptor Antagonist Data

ligand	binding affinities ($pA_2 \pm$ SEM)
1	6.8 ± 0.2
13d	7.2 ± 0.2
13e	6.8 ± 0.4

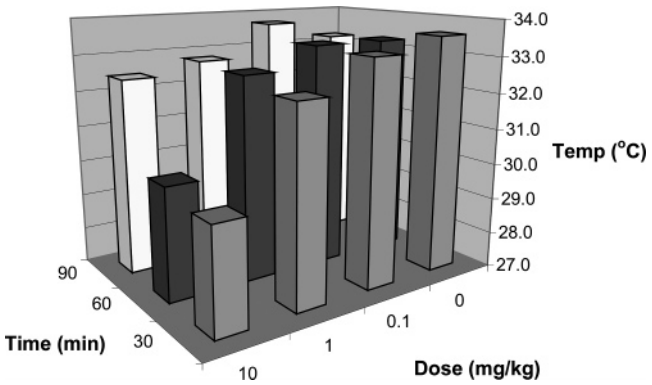

Figure 3. Hypothermia produced by **13e** following ip administration in mice. Data represent the mean core body temperature (in °C) of mice.

efficacy of **13e** at M_1 receptors was comparable to that of **1** (31% ± 6.5 and 47% ± 4.4, respectively). Removal of the terminal thiadiazole moiety as found in **3** resulted in a further decrease in binding affinity across M_1 to M_5 receptor subtypes (Figure 1), with the lowest binding affinity at M_5 receptors, indicating the importance of the terminal thiadiazole moiety. Both compounds **3** and **13e** showed a very weak activity at M_5 receptors, which may indicate potential utility in the treatment of schizophrenia, since blocking the M_5 receptor should decrease dopamine release.

In these series of compounds, **1**, **3**, and **13e** all lack functional activity at the M_3 receptors, indicating minimal potential for M_3 receptor-mediated side effects. In fact, using pharmacological screens in mice, it was shown that M_3-mediated side effects (i.e., diarrhea, salivation, and lacrimation) were found to be minimal for **13e** at doses up to 10 mg/kg ip (data not shown). Compounds **13e** and **13d** were further evaluated for their functional antagonism properties using inhibition of carbachol at the M_3 receptor. Both **13e** and **13d** shifted the dose−response curve of carbachol to the right, consistent with antagonist properties. From these data, pA_2 values of 6.8 (**13e**) and 7.2 (**13d**) were calculated (Table 5).

As far as binding affinity at M_2 and M_4 receptors, the substitution of the terminal 1,2,5-thiadiazole in **1** with 1,2,4-thiadiazole in **13e** resulted in a significant decrease in the binding affinity. However, at M_2 receptors, **13e** exhibited a dramatic decrease in agonist potency but with comparable efficacy at 6.6 and 101%, respectively, as compared to 9.3 and 118% for **1**. Consequently, **13e** produced slightly less hypothermia (Figure 3) than **1** at 10 mg/kg dose 1 h after ip administration. This suggests that **13e**, similar to **1**, is able to penetrate into the brain as an M_2 agonist.[26] Interestingly, even with a significant decrease in M_4 binding affinity and dramatic decrease in functional potency, **13e** exhibited the highest M_4 agonist efficacy with 148% of the carbachol response. Although **1** has the highest M_4 binding affinity and functional potency, it exhibited a modest agonist efficacy at 40%; moreover, removal of the 1,2,5-thiadiazole moiety, as found in **3**, resulted in a dramatic decrease in potency of about 2 orders of magnitude.

These results suggest that the positioning of the methoxy group on the thiadiazole moiety may play a crucial role in M_2 and M_4 affinity and activity. Furthermore, this suggests that **13e** might offer similar utility in treating the cognitive deficits associated with schizophrenia with possible fewer M_2 and M_3 side effects than **1**.

Table 6. Inhibition of [^{3}H]-(*R*)-QNB Binding to Wild-Type and Chimeric Receptors Expressed as pK_i Values[a]

ligand	M_1 (WT)	M_1 ($o2M_5$)	M_1 ($o3M_5$)	M_1 ($o2/o3M_5$)	M_5 (WT)
carbachol	5.9 ± 0.1	4.7 ± 0.0	4.9 ± 0.1	4.2 ± 0.0	4.7 ± 0.3
xanomeline	6.8 ± 0.0	6.2 ± 0.5	6.3 ± 0.1	5.9 ± 0.2	5.8 ± 0.1
2c	10 ± 0.2	7.4 ± 0.0	7.7 ± 0.1	7.0 ± 0.1	7.2 ± 0.0
1	7.3 ± 0.2	6.7 ± 0.0	6.9 ± 0.1	6.5 ± 0.1	6.4 ± 0.3

[a] Data represent the mean (±SEM from three assays, each performed in triplicate. Note that the data for carbachol and xanomeline at M_1 receptors were collected at different times and with different receptor expression levels as compared with data presented in Table 1.

Chimeric and Mutant Receptors. The interaction of muscarinic agonists with transmembrane domain amino acid residues was evaluated by examining receptor binding properties at wild-type and mutant (Thr192Ala) M_1 receptors. Previous studies had identified Thr192 as an important amino acid residue involved in the binding of small muscarinic agonists such as acetylcholine and carbachol.[31] The binding affinities of carbachol, xanomeline, and **2c** were examined at wild-type and mutant (Thr192Ala) M_1 receptors. As found previously, carbachol exhibited lower affinity for (Thr192Ala) M_1 receptors (pK_i of 2.7 ± 0.2) than for wild-type M_1 receptors (pK_i of 5.7 ± 0.1). Xanomeline also displayed lower affinity for (Thr192Ala) M_1 receptors (pK_i of 5.4 ± 0.1) than for wild-type M_1 receptors (pK_i of 7.9 ± 0.3). In a similar fashion, **2c** displayed lower affinity for (Thr192Ala) M_1 receptors (pK_i of 7.0 ± 0.1) than for wild-type M_1 receptors (pK_i of 9.9 ± 0.3). The data suggest that xanomeline and **2c** interact with transmembrane domains of M_1 receptors in a similar fashion to smaller molecules. Their relatively high affinity for M_1 receptors may also depend on interaction with residues outside of the common binding site for agonists located within the transmembrane domain.

In order to assess this possibility, chimeric receptors were developed. Exchange of the second (o2) extracellular loop of the M_1 receptor with the corresponding sequence from M_5 receptors lowered the binding affinity and activity of both compounds **1** and **2c** (see Figure 7 and Table 6). The activities of carbachol and xanomeline were relatively unchanged, although the potency of xanomeline was decreased (see Figure 7 and Table 7). The o2 loop may play a role in the binding and activity of relatively large muscarinic agonists such as **1** and **2c**.

Exchange of the third (o3) extracellular loop of the M_1 receptor with the corresponding sequence from M_5 receptors dramatically lowered the activity of xanomeline, **1** and **2c**. The third extracellular loop of M_1 receptors therefore may interact with functional groups common to xanomeline, **1**, and **2c**. Replacement of both the o2 and o3 loops of the M_1 receptor with the corresponding sequences from M_5 receptors virtually eliminated agonist activity for **1** and **2c**. The data strongly suggest that **1** and **2c** interact with the second and third extracellular domains of M_1 receptors and that these interactions are important for conferring agonist activity and selectivity.

On the basis of the data from chimeric M_1/M_5 receptors, it was hypothesized that mutation of individual amino acid residues in the second and/or third extracellular loops would result in a loss of binding affinity or agonist activity at residues that are involved in the binding of **1** and **2c**. In contrast, smaller agonists such as carbachol should not be dramatically affected

Table 7. Stimulation of Phosphoinositide Metabolism by Muscarinic Agonists at Wild-Type and Chimeric Muscarinic Receptors[a]

	M_1 (WT)		M_1 ($o2M_5$)		M_1 ($o3M_5$)		M_1 ($o2/o3M_5$)		M_5 (WT)	
ligand	pEC_{50}	S_{max} (%)	pEC_{50}	S_{max} (%)	pEC_{50}	S_{max} (%)	pEC_{50}	S_{max} (%)	pEC_{50}	S_{max} (%)
carbachol	4.9 ± 0.0	100 ± 12	6.0 ± 0.1	100 ± 9.0	5.0 ± 0.2	100 ± 8.0	4.1 ± 0.2	100 ± 2.0	5.2 ± 0.3	100 ± 12
xanomeline	8.0 ± 0.0	79 ± 12	6.2 ± 0.2	75 ± 16	5.2 ± 0.1	21 ± 2.0	6.5 ± 0.0	20 ± 1.0	5.6 ± 0.2	46 ± 7.5
2c	8.1 ± 0.1	69 ± 12	7.1 ± 0.3	34 ± 11	6.2 ± 0.4	23 ± 4.0	−	2.0 ± 1.0	−	na
1	7.6 ± 0.3	40 ± 3.7	7.1 ± 0.3	20 ± 7.0	7.0 ± 0.2	9.7 ± 2.2	−	5.3 ± 2.2	3.7 ± 2.1	14 ± 7.8

[a] Data represent the mean (±SEM) from three assays, each performed in triplicate. The functional data for xanomeline were collected at different times using different receptor expression levels, resulting in slightly different values as compared with Table 3. Wild-type M_1 and chimeric receptors were compared using similar levels of receptor expression.

Table 8. Stimulation of Phosphoinositide Metabolism by Selected Muscarinic Agonists at Wild-Type and Mutant Muscarinic Receptors[a]

	M_1(WT)		M_1(E170K)		M_1(Q185E)		M_5(WT)	
ligand	pEC_{50}	S_{max}	pEC_{50}	S_{max}	pEC_{50}	S_{max}	pEC_{50}	S_{max}
carbachol	4.9 ± 0.0	100 ± 12	4.8 ± 0.1	100 ± 9.0	4.8 ± 0.1	100 ± 11	5.2 ± 0.3	100 ± 12
xanomeline	8.0 ± 0.0	79 ± 12	6.8 ± 0.1	31 ± 6.0	6.8 ± 0.2	86 ± 14	5.6 ± 0.2	46 ± 7.5
2c	8.1 ± 0.1	69 ± 12	8.0 ± 0.4	66 ± 13	7.3 ± 0.1	50 ± 13	−	na
1	7.6 ± 0.3	40 ± 3.7	5.7 ± 0.1	27 ± 1.8	6.6 ± 0.2	14 ± 3.3	3.7 ± 2.1	14 ± 7.8

[a] Data represent the mean (±SEM) from three experiments, each performed in triplicate.

by such mutations, since they interact primarily with highly conserved residues within the transmembrane domains. Thus, carbachol served as a useful control for comparing the effects of individual mutations. Xanomeline also served as a helpful control, since it shares many structural features with **1** and **2c**.

The first set of site-directed mutagenesis studies examined the effects of replacing the four nonconserved residues located in the third extracellular loop of M_1 receptors with the corresponding residues of M_5 receptors. No significant differences were noted in the binding or activity of the mutant receptors (data not shown). A second set of studies focused on replacing residues found in the second extracellular loop of M_1 receptors with the corresponding residues of M_5 receptors. Two mutant M_1 receptors were created and characterized M_1(E170K) and M_1(Q185E). As summarized in Table 8, the data indicate that while carbachol activity remained unaffected, mutation of Glu170 and Gln185 to the corresponding M_5 residues lowered the potency and activity of **1**. Therefore, both residues appear to contribute to the potency and activity of **1** at M_1 receptors as compared with M_5 receptors. The data suggest that derivatives of compound **1** containing hydrogen-bond donors (e.g., primary amines or amides) will exhibit even better functional selectivity for M_1 vs M_5 receptors. This hypothesis can be tested by synthesizing and characterizing new ligands incorporating hydrogen-bond-donating groups attached to the terminal 1,2,5-thiadiazole moiety found in **1**.

Using molecular modeling, the effect of spacer length and the interactions of the terminal thiadiazoles were further studied for the M_1 wild-type (WT) receptor and for the o2 and o3 chimeric receptors. Table 4 summarizes the $O_\alpha \cdots O_\omega$ distances optimized for the ligand bound to the receptor for the dicationic (**2c**) and for the monocationic (**1** and **13e**) compounds. The values for the bound **2c** dication are generally larger than 9.7 ± 0.9 Å, calculated in the model saline solution. In contrast, the $O_\alpha \cdots O_\omega$ distances for monocations are nearly in the range of 11.1 ± 1.7 Å obtained for **1** also in solution. Calculated values indicate that ligands with $n = 3$ spacer units need not undergo large $O_\alpha \cdots O_\omega$ stretching in order to adopt a structure favorable for the binding to the receptor.

Each of the three ligands form a strong, $N-H^+ \cdots {}^-OCO$ hydrogen bond between the ligand's protonated tetrahydropyridine site and the carboxylate group of Asp105 of TM3 located at a depth of about 11 Å from the loop domain (Table 4). The only exception was found for **1** in the o2+o3 mutant receptor, where the hydrogen bond increased from 1.68 to 5.06 Å throughout the last 400 ps of the calculations. This finding was primarily attributed to the effect of the mutations in the o2 loop, which probably allows more libration and translation for the ligand.

Hydrogen-bond formation was found possible between the side chains of some loop residues and the ionic and polar sites of **2c** and **1**, respectively. However, no hydrogen bond to the 3-methoxy-1,2,4-thiadiazole ring of **13e** was predicted in this area. An important competitor to the protein−ligand hydrogen bond formation in this region is the possible Lys392···Glu397 salt bridge in the WT and the o2 chimeric receptors. The calculations predict the presence of this type of salt bridge only in the case of the o2 chimeric receptor, whereas no salt bridge was found in the WT receptor (Table 4). This difference has been considered as a remarkable conformational difference between the WT and o2 receptors. The larger flexibility of the ligand in the o2 mutant receptor, as mentioned above, results in the increase of the optimized length of the hydrogen bond of **2c** to Glu397 from 1.71 to 4.34 Å throughout the last 400 ps of the simulation.

A second support for the relevance of the conformational difference between the WT and o2 receptors is that the methoxy group of **1** forms a weak hydrogen bond to Lys392 only when the ligand is bound to the o2 receptor. The Lys392···Gly397 salt bridge does not prevent the formation of the protein−ligand hydrogen bond in this case. The position of the methoxy group seems to be important, however, because no methoxy···lysine hydrogen bond with the isomeric **13e** ligand was revealed from the calculations.

For the o3 chimeric receptor, the 392 and 397 residues are Asp and Val without the possibility for salt-bridge formation. For this receptor, however, Asp392 forms a strong hydrogen bond with the second protonated tetrahydropyridine site of the dicationic **2c**. The Lys393 residue can interact with the polar but neutral site of **1** through a weak $N-H^+ \cdots OCH_3$ hydrogen bond (the 200-ps bond length was 2.05 Å). The position of the methoxy group is crucial again, because no hydrogen bond to Lys393 was calculated with the **13e** ligand. Finally, the interesting case of the o2+o3 double loop-mutation was studied for two prototypes, **2c** and **1**. Although the $O_\alpha \cdots O_\omega$ separation is within the range found in other cases in this study, the hydrogen bond with Asp105 was maintained only for **2c** in the depth of the receptor (see above). The double loop-mutation removed all ionic and polar side chains in the investigated domain, so the head groups of the bivalent ligands did not find

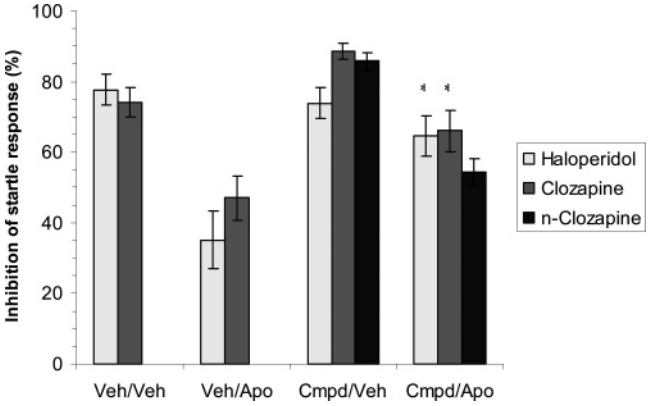

Figure 4. Haloperidol and clozapine (both at 1.0 mg/kg) reversed the effects of apomorphine (Apo) on the prepulse inhibition of the startle response. *N*-Desmethylclozapine was ineffective at 1.0 mg/kg. *, $p < 0.05$.

a partner for hydrogen-bond formation. As a least unfavorable arrangement, the ring sites are accommodated in a hydrophobic pocket allowing for intense van der Waals interactions.

Effect of Spacer and Terminal Thiadiazole. Considering their selectivity and activity, **1** and **13e** were subjected to further structural modifications. The correlation between the potency of the compounds to the overall lipophilicity and flexibility of the linker was also investigated by using a tripropylene glycol spacer. For the corresponding pair **1** and **18a**, the replacement of the spacer with tripropylene glycol resulted in relatively lower binding affinity at M_2, M_3, and M_4 receptors with a dramatic decrease observed at the M_4 receptor (Table 2). For the corresponding pair **13e** and **18b**, a relative increase in M_1 affinity and a decrease in M_4 affinity were observed. Compound **18b** resulted in an interesting functional activity profile in that it is essentially inactive at M_2, M_3, and M_5 receptors but exhibited modest efficacy at M_1 receptors and relatively high efficacy at M_4 receptors (Table 3). Thus, **18b** appears to be a functionally selective M_4 agonist.

Behavioral Studies. Antipsychotic activity was assessed by measuring the ability of compounds to reverse the effects of apomorphine on prepulse inhibition of the startle response. The paradigm serves as a measure of sensory motor gating deficits—deficits associated with schizophrenia.[21] A brief tone presented immediately prior to a startle stimulus (e.g., loud noise) dampens the startle response. The dopamine agonist apomorphine limits the impact of the tone on the startle response (Figure 4). To verify the validity of the paradigm to identify antipsychotic activity, the classical antipsychotic haloperidol and the atypical antipsychotic clozapine were examined in the prepulse inhibition paradigm. Both antipsychotics reversed the effects of apomorphine on the prepulse inhibition of the startle response (Figure 4). In contrast, the clozapine metabolite *N*-desmethylclozapine and xanomeline, an M_1 and M_4 agonist, did not reverse the effects of apomorphine on the prepulse inhibition of the startle response (Figures 4 and 5).

Compound **1** reversed the effects of apomorphine on the prepulse inhibition of the startle response at doses of 1.0 and 3.0 mg/kg (Figure 6). Since **1** displays activity at M_1, M_2, and M_4 receptors, the data suggest that M_2 activity may be an important factor for the ability of muscarinic agonists to exhibit antipsychotic activity. These data indicate that **1** has the potential to treat psychotic symptoms associated with schizophrenia.

Conclusions

In conclusion, the initial SAR studies of the new class of muscarinic agonists conducted to identify more subtype-selective

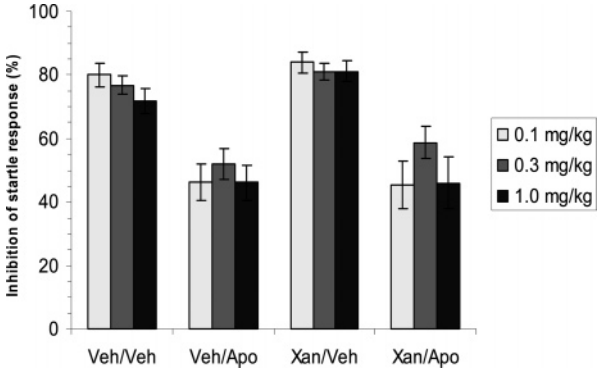

Figure 5. Xanomeline (Xan) did not reverse the effects of apomorphine on the prepulse inhibition of the startle response.

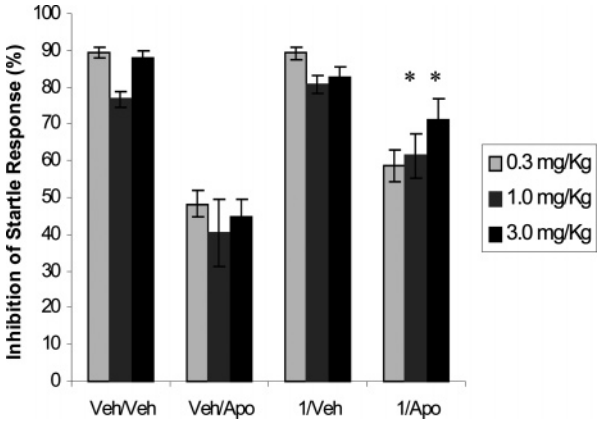

Figure 6. Compound **1** reversed the effects of apomorphine on the prepulse inhibition of the startle response. *, $p < 0.05$.

compounds compared to **1** led to the identification of **13e**, which might offer similar utility in treating the cognitive deficits associated with schizophrenia with possibly fewer M_2 and M_3 side effects. In addition, the distance of the terminal thiadiazole and the positioning of the methoxy group can increase binding affinity for certain mAChRs subtypes (e.g., M_2 receptors for **13d** and M_4 receptors for **1**) and enhance functional efficacy at M_4 for **13e** and **18b**. In addition, **13e** exhibited significant functional selectivity for M_1 receptors versus M_5 receptors. Compound **18b** resulted in an interesting functional activity profile with modest functional efficacy at M_1 receptors and relatively high efficacy at M_4 receptors. The modeling results are in line with the experimental finding that the o2 and/or o3 mutations weaken the receptor−ligand interactions. Further SAR studies around the terminal thiadiazole as well as the tetrahydropyridine moiety are in progress.

Experimental Section

Chemistry. Reactions were carried out under nitrogen. Melting points were determined on a Fisher-Johns melting point apparatus and are presented uncorrected. ^1H and ^{13}C NMR spectra were obtained with a Bruker ACF 400-MHz spectrometer. Elemental analyses (C, H, N) were performed by Atlantic Microlab, Inc., GA; the analytical results were within 0.4% of the theoretical values for the formula given (except for **18b**, where results were within 0.47%). Precoated silica gel GHLF uniplates (250 μm), purchased from Analtech, Inc., were used for TLC, and spots were examined with UV light at 254 nm or iodine vapor. Column chromatography purification was performed on Davisil silica gel 200−425 mesh obtained from Fisher Scientific. Tetrahydrofuran (THF) was dried over sodium benzophenone ketyl and distilled. All other commercially available solvents and reagents were used without further

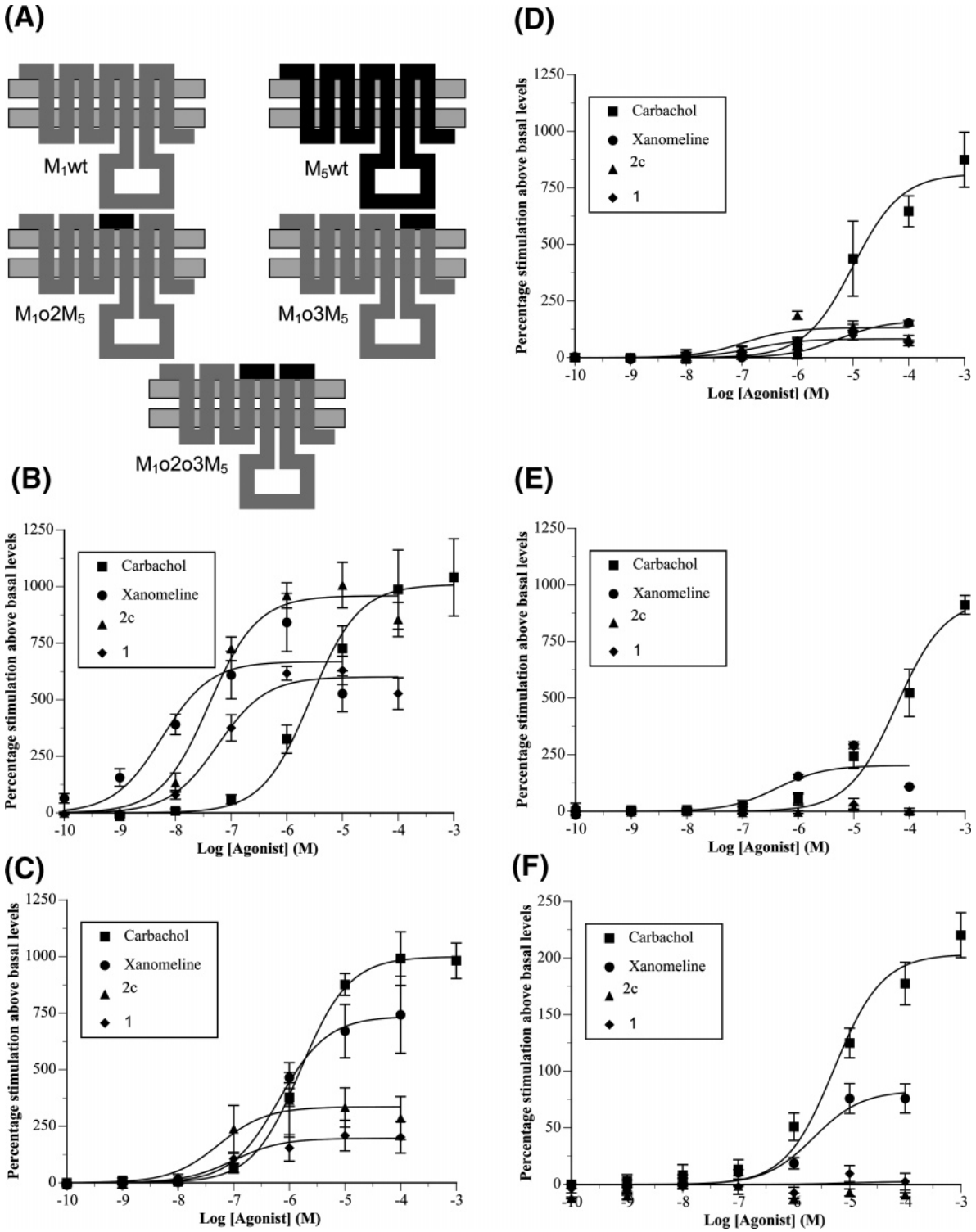

Figure 7. Stimulation of phosphoinositide metabolism at wild-type and chimeric muscarinic receptors expressed in A9 L cells: (A) schematic depiction of M_1 (gray), M_5 (black) and chimeric receptors, (B) wild-type M_1 receptors, (C) $M_1(o2M_5)$ receptors, (D) $M_1(o3M_5)$ receptors, (E) $M_1(o2o3M_5)$ receptors, and (F) wild-type M_5 receptors.

purification unless otherwise specified. No particular attempts were made to optimize reaction conditions for most of the reactions described.

The key starting materials (Figure 1B), 3-(3-chloro-1,2,5-thiadiazol-4-yl)pyridine (**4**), 3-chloro-4-methoxy-1,2,5-thiadiazole (**5**), and 5-chloro-3-methoxy-1,2,4-thiadiazole (**6**) were synthesized using published procedures.[26−28] The various ethylene glycol spacers were commercially available, while the tripropylene glycol spacer (**7**) was prepared from 1,3-propanediol.[29] All other commercially available solvents and reagents were used without further purification unless otherwise specified.

General Procedure for the Preparation of Di(ethylene glycol)-ethyl [3-(Pyrid-3-yl)-1,2,5-thiadiazol-4-yl] Ether (9a). A suspension of 60% NaH in mineral oil (890 mg, 22.2 mmol) was washed with anhydrous hexane and suspended in freshly distilled THF (30 mL). Then, **8a** (2.15 g, 20.2 mmol) in THF (100 mL) was added to the above suspension and the reaction mixture was refluxed for 1 h. Compound **4** (1.0 g, 5.1 mmol) in THF (100 mL) was added, and the reaction mixture was refluxed for 24 h. The mixture was evaporated under a vacuum and quenched with ice water (50 mL). The aqueous solution was extracted twice with $CHCl_3$. The combined organic extract was washed with brine, dried over

anhydrous Na_2SO_4, and concentrated to yield the crude compound. After silica gel chromatography with $CHCl_3$/MeOH (97:3), **9a** was obtained as a pale yellow solid (1.30 g, 96.1%): mp 53−56 °C; R_f = 0.22 [$CHCl_3$/MeOH (97:3)]; ^{1}H NMR ($CDCl_3$) δ 3.70−3.85 (m, 4H), 3.96−4.00 (m, 2H), 4.69−4.74 (m, 2H), 7.50−7.56 (m, 1H), 8.56 (d, J = 8.2 Hz, 1H), 8.67 (dd, J = 1.4 and 5.0 Hz, 1H), 9.54 (s, 1H); ESI-MS *m*/*z* 268.0 [M + H$^+$], 290.0 [M + Na].

Tri(ethylene glycol)ethyl [3-(Pyrid-3-yl)-1,2,5-thiadiazol-4-yl] Ether (9b). Compound **9b** was prepared from **4** (1.0 g, 5.0 mmol), **8b** (3.04 g, 20.2 mmol), and NaH (0.89 g, 22.2 mmol) using a procedure similar to that described earlier to afford the title compound as a yellow oil (1.72 g, 21%): R_f = 0.14 [$CHCl_3$/MeOH (97:3)]; ^{1}H NMR ($CDCl_3$) δ 3.59−3.63 (m, 2H), 3.68−3.75 (m, 6H), 3.89−3.92 (m, 2H), 4.65−4.67 (m, 2H), 7.39−7.42 (m, 1H), 8.41 (d, J = 8.0 Hz, 1H), 8.60 (dd, J = 1.6 and 5.2 Hz, 1H), 9.46 (s, 1H); ESI-MS *m*/*z* 312.1 [M + H$^+$], 334.0 [M + Na].

Penta(ethylene glycol)ethyl [3-(Pyrid-3-yl)-1,2,5-thiadiazol-4-yl] Ether (9d). Compound **9d** was prepared from **4** (1.0 g, 5.0 mmol), **8d** (3.04 g, 20.2 mmol), and NaH (0.89 g, 22 mmol) using a procedure similar to that described earlier to afford the title compound as a yellow oil (1.72 g, 85%): R_f = 0.17 [$CHCl_3$/MeOH (95:5)]; ^{1}H NMR ($CDCl_3$) δ 3.59−3.76 (m, 16H), 3.94−3.99 (m, 2H), 4.69−4.74 (m, 2H), 7.53−7.59 (m, 1H), 8.60 (d, J = 8.0 Hz, 1H), 8.70 (d, J = 1.6 and 5.0 Hz, 1H), 9.44 (s, 1H); ESI-MS *m*/*z* 400.2 [M + H$^+$], 422.1 [M + Na].

Tri(propylene glycol)ethyl [3-(Pyrid-3-yl)-1,2,5-thiadiazol-4-yl] Ether (14). Compound **14** was prepared from **4** (0.60 g, 3.0 mmol), **7** (1.70 g, 8.8 mmol), and NaH (0.42 g, 10 mmol) using a procedure similar to that described earlier to afford the title compound as a yellow oil (0.59 g, 54% yield): R_f = 0.42 [CH_2Cl_2/MeOH (90:10)]; ^{1}H NMR ($CDCl_3$) δ 1.80−1.86 (m, 4H), 2.15−2.18 (m, 2H), 3.49−3.53 (m, 4H), 3.58−3.67 (m, 4H), 3.74−3.78 (m, 2H), 4.62−4.66 (m, 2H), 7.39−7.42 (m, 1H), 8.41 (d, J = 8.0 Hz, 1H), 8.64 (dd, J = 1.6 and 4.8 Hz, 1H), 9.39 (s, 1H); ^{13}C NMR ($CDCl_3$) 29.52, 30.20, 32.23, 62.21, 67.47, 68.18, 68.37, 68.78, 70.42, 123.70, 127.91, 135.06, 145.18, 148.72, 150.35, 162.91.

General Procedure for the Preparation of Di(ethylene glycol)-(3-methoxy-1,2,5-thiadiazol-4-yl) [3-(Pyrid-3-yl)-1,2,5-thiadiazol-4-yl] Ether(10a). A suspension of 60% NaH (220 mg, 5.5 mmol) in mineral oil was washed with anhydrous hexane and suspended in freshly distilled THF (30 mL). Then, **9a** (0.75 g, 2.8 mmol) in THF (30 mL) was added to the above suspension. The reaction mixture was refluxed for 30 min. Compound **5** (0.63 g, 4.21 mol) in THF (30 mL) was added, and the reaction mixture was refluxed for 24 h. The mixture was evaporated under vacuum and quenched with ice water (20 mL), and the aqueous solution was extracted twice with $CHCl_3$. The combined organic extract was washed with water, dried over anhydrous Na_2SO_4, and concentrated to yield the crude compound. After silica gel chromatography with CH_2Cl_2/MeOH (100:3), **10a** was obtained as a yellow solid (0.526 g, 49%): R_f = 0.21 [CH_2Cl_2/MeOH (100:3)]; ^{1}H NMR ($CDCl_3$) δ 3.87−3.89 (t, 2H), 3.91−3.93 (t, 2H), 3.96 (s, 3H), 4.50−4.52 (t, 2H), 4.62−4.64 (t, 2H), 7.29−7.32 (m, 1H), 8.35 (d, J = 8.0 Hz, 1H), 8.56 (d, J = 4.0 Hz, 1H), 9.31 (s, 1H); ^{13}C NMR ($CDCl_3$) δ 57.6, 69.3, 69.4, 69.8, 70.2, 123.5, 127.6, 134.8, 145.2, 148.8, 150.2, 151.5, 151.4, 162.6.

Tri(ethylene glycol)(3-methoxy-1,2,5-thiadiazol-4-yl) [3-(Pyrid-3-yl)-1,2,5-thiadiazol-4-yl] Ether (10b). Compound **10b** was prepared from **9b** (0.317 g, 1.02 mmol), **5** (0.23 g, 1.53mmol), and NaH (0.081 g, 2.0 mmol) using a procedure similar to that described earlier to afford the title compound as a yellow oil (0.17 g, 18%): R_f = 0.52 [CH_2Cl_2/MeOH (95:5)]; ^{1}H NMR ($CDCl_3$) δ 3.48 (s,-2H), 3.76 (s, 2H), 3.86−3.88 (m, 2H), 3.94−3.96 (m, 2H), 4.05 (s, 3H), 4.51−4.54 (m, 2H), 4.70−4.72 (m, 2H), 7.78−7.82 (m, 1H), 8.69 (d, J = 8.0 Hz, 1H), 8.92 (dd, J = 1.6 and 5.2 Hz, 1H), 9.52 (s, 1H); ^{13}C NMR ($CDCl_3$) 57.6, 69.3, 69.4, 69.8, 70.4, 70.9, 71.0, 123.6, 127.7, 135.1, 145.1, 148.6, 150.1, 151.6, 152.4, 162.6.

Penta(ethylene glycol)(3-methoxy-1,2,5-thiadiazol-4-yl) [3-(Pyrid-3-yl)-1,2,5-thiadiazol-4-yl] Ether (10d). Compound **10d** was prepared from **9d** (0.72 g, 1.80 mmol), **5** (0.41 g, 2.7 mmol), and NaH (0.14 g, 3.6 mmol) using a procedure similar to that described earlier to afford the title compound as yellow oil (0.17 g, 18%): R_f = 0.11 [CH_2Cl_2/MeOH (100:3)]; ^{1}H NMR ($CDCl_3$) δ 3.61−3.71 (m, 12H), 3.82−3.85 (m, 2H), 3.91−3.93 (m, 2H), 4.06 (s, 3H), 4.51−4.54 (m, 2H), 4.65−4.67 (m, 2H), 7.36−7.39 (m, 1H), 8.40 (d, J = 8.0 Hz, 1H), 8.62 (dd, J = 1.6 and 4.8 Hz, 1H), 9.37 (s, 1H); ^{13}C NMR ($CDCl_3$) 62.23, 69.38, 69.93, 70.46, 70.78, 70.83, 70.85, 70.87, 70.91, 70.98, 123.61, 127.75, 134.98, 145.31, 148.96, 150.39, 151.71, 152.54, 162.74.

Tri(propylene glycol)(3-methoxy-1,2,5-thiadiazol-4-yl) [3-(Pyrid-3-yl)-1,2,5-thiadiazol-4-yl] Ether (15a). Compound **15a** was prepared from **14** (0.32 g, 1.0 mmol), **5** (0.27 g, 2.0 mmol), and NaH (0.07 g, 2.0 mmol) using a procedure similar to that described earlier to afford the title compound as a yellow oil (0.126 g, 29%): R_f = 0.60 [$CHCl_3$/MeOH (95:5)]; ^{1}H NMR ($CDCl_3$) δ 1.80−1.83 (m, 2H), 2.04−2.10 (m, 2H), 2.12−2.28 (m, 2H), 3.47−3.55 (m, 6H), 3.59−3.62 (t, 2H), 4.09 (s, 3H), 4.46−4.50 (t, 2H), 4.61−4.64 (t, H), 7.38−7.41 (m, 1H), 8.41 (d, J = 8.0 Hz, 1H), 8.64 (dd, J = 1.6 and 4.8 Hz, 1H), 9.39 (s, 1H); ^{13}C NMR ($CDCl_3$) δ 29.44, 29.58, 30.25, 57.72, 67.25, 67.39, 68.03, 68.19, 68.81, 123.63, 127.86, 134.92, 145.20, 148.85, 150.40, 151.88, 152.56, 162.92.

General Procedure for the Preparation of Di(ethylene glycol)-(3-methoxy-1,2,5-thiadiazol-4-yl) [3-(1-Methyl-1,2,5,6-tetrahydropyrid-3-yl)-1,2,5-thiadiazol-4-yl] Ether (12a). To a solution of **10a** (0.526 g, 1.37 mmol) in acetone (10 mL) and $CHCl_3$ (5 mL) was added CH_3I (6 mL, 96 mmol), the solution was stirred under nitrogen for 4 days at room temperature, and the reaction was monitored by TLC. The residual quaternary iodide **11a** was obtained by removing the solvents under reduced pressure to afford a pale yellow solid and was used immediately without further purification: R_f = baseline [CH_2Cl_2/MeOH (100:3)];^{1}H NMR ($CDCl_3$) 3.98−4.00 (m, 2H), 4.02 (s, 3H, OCH_3), 4.04−4.06 (m, 2H), 4.59−4.61 (m, 2H), 4.75−4.76 (m, 3H), 4.78 (s, 3H, NCH_3), 8.24−8.27 (m, 1H), 9.15 (d, J = 8.4 Hz, 1H), 9.51 (s, 1H), 9.53 (s, 1H). The pyridinium iodide **11a** (550 mg, 1.38 mmol) was dissolved in a mixture of CH_3OH (10 mL) and $CHCl_3$ (10 mL). The solution was cooled to 0−5 °C, and $NaBH_4$ (210 mg, 5.55 mmol) was added. After the mixture was stirred at 0−5 °C for 1 h, another 210 mg of $NaBH_4$ was added, followed by another 210 mg after 1 h. The reaction continued for 2 h. Ice water was added to the reaction mixture, which was then extracted twice with $CHCl_3$. The combined organic extract was washed with water, dried over anhydrous Na_2SO_4, and concentrated to give the crude compound. After the silica gel chromatography with CH_2Cl_2/MeOH (97:3), **12a** was obtained as a yellow oil (141 mg, 25%): R_f = 0.10 [CH_2Cl_2/MeOH (97:3)]; ^{1}H NMR ($CDCl_3$) δ 2.39−2.43 (m, 2H), 2.45 (s, 3H), 2.54−2.56 (t, 2H), 3.43 (m, 2H), 3.91−3.95 (m, 4H), 4.08 (s, 3H), 4.55−4.58 (m, 2H), 4.60−4.63 (m, 2H), 7.05−7.07(m, 1H); ^{13}C NMR ($CDCl_3$) δ 26.81, 46.13, 51.45, 55.22, 57.68, 69.28, 69.55, 69.92, 69.94, 128.90, 147.16, 151.63, 162.34, 194.79.

Tri(ethylene glycol)(3-methoxy-1,2,5-thiadiazol-4-yl) [3-(1-Methyl-1,2,5,6-tetrahydropyrid-3-yl)-1,2,5-thiadiazol-4-yl] Ether (12b). Compound **11b** was prepared from **10b** (84 mg, 0.197 mmol) and CH_3I (3 mL, 48 mmol) using a procedure similar to that described earlier to provide the pyridinium iodide compound as a yellow oil: R_f = baseline [CH_2Cl_2/MeOH (100:3)]; ^{1}H NMR ($CDCl_3$) δ 3.72−3.77 (m, 4H), 3.83−3.96 (t, 2H), 3.98−4.00 (t, 2H), 4.05 (s, 3H, OCH_3), 4.47−4.50 (t, 2H), 4.72−4.74 (t, 2H), 4.79 (s, 3H, NCH_3), 8.24 (m, 1H), 9.12 (d, J = 8.4 Hz, 1H), 9.51 (s, 1H), 9.53 (s, 1H). The pyridinium iodide **11b** (98 mg, 0.172 mmol) was reduced with $NaBH_4$ (26 mg, 0.687 mmol) using a procedure similar to that described earlier to afford the title compound **12b** as brown oil (50 mg, 57%): R_f = 0.13 [CH_2Cl_2/MeOH (95:5)]; ^{1}H NMR ($CDCl_3$) δ 2.42−2.44 (m, 5H), 2.53−2.56 (t, 2H), 3.43 (s, 2H), 3.70 (s, 4H), 3.86−3.90 (m, 4H), 4.08 (s, 3H), 4.54−4.61 (m, 4H), 7.07−7.09 (m, 1H); ^{13}C NMR ($CDCl_3$) δ 26.69,46.03, 51.37, 57.66, 69.31, 69.50, 69.88, 70.01, 70.89, 71.00, 128.84, 129.25, 147.05, 151.67, 152.53, 162.39, 194.79.

Penta(ethylene glycol)(3-methoxy-1,2,5-thiadiazol-4-yl) [3-(1-Methyl-1,2,5,6-tetrahydropyrid-3-yl)-1,2,5-thiadiazol-4-yl] Ether (12d). Compound **11d** was prepared from **10d** (170 mg, 0.331

mmol) and CH_3I (3 mL, 48 mmol) using a procedure similar to that described earlier to provide the pyridinium iodide as a yellow oil: R_f = baseline [CH_2Cl_2/MeOH (100:3)]; ^{1}H NMR ($CDCl_3$) δ 3.54−3.70 (m, 10H), 3.76−3.78 (m, 2H), 3.84−3.87 (m, 2H), 4.00−4.02 (m, 2H), 4.07 (s, 3H, OCH_3), 4.54−4.57 (t, 2H), 4.74−4.76 (t, 2H), 4.79 (s, 3H, NCH_3), 8.18−8.22 (m, 1H), 8.12−9.14 (d, J = 8.4 Hz, 1H), 9.44−9.47 (d, J = 5.6 Hz, 1H), 9.59 (s, 1H). The pyridinium iodide **11d** (190 mg, 0.289 mmol) was reduced with $NaBH_4$ (120 mg, 3.17 mmol) using a procedure similar to that described earlier to afford the title compound **12d** as a yellow oil (91 mg, 51%): R_f = 0.28 [CH_2Cl_2/MeOH (97:3)]; ^{1}H NMR ($CDCl_3$) δ 2.49−2.51 (m, 5H), 2.63−2.66 (t, 2H), 3.52 (s, 2H), 3.62−3.68 (m, 12H), 3.84−3.89 (m, 4H), 4.07 (s, 3H), 4.52−4.55 (m, 2H), 4.57−4.60 (m, 2H), 7.09−7.11 (m, 1H); ^{13}C NMR ($CDCl_3$) δ 26.44, 45.85, 51.30, 54.87, 57.68, 69.25, 69.44, 69.95, 70.08, 70.81, 70.86, 70.88, 70.91, 70.93, 128.71, 128.78, 146.79, 151.70, 152.54, 162.39.

Tri(propylene glycol)(3-methoxy-1,2,5-thiadiazol-4-yl) [3-(1-Methyl-1,2,5,6-tetrahydropyrid-3-yl)-1,2,5-thiadiazol-4-yl] Ether (17a). Compound **16a** was prepared from **15a** (126 mg, 0.342 mmol) and CH_3I (2 mL, 32 mmol) using a procedure similar to that described earlier to provide the title compound as a yellow solid: R_f = 0.37 [CH_2Cl_2/MeOH (90:10)]; ^{1}H NMR ($CDCl_3$) δ 1.79−1.81 (m, 2H), 2.05−2.07 (m, 2H), 2.18−2.20 (m, 2H), 3.46−3.54 (m, 6H), 3.59−3.61 (t, 2H), 4.09 (s, 3H, OCH_3), 4.45−4.48 (t, 2H), 4.69−4.71 (t, 2H), 4.77 (s, 3H, NCH_3), 8.22−8.24 (m, 1H), 9.14 (d, J = 8.4 Hz, 1H), 9.39 (s, 1H), 9.57 (d, J = 6 Hz, 1H). The pyridinium iodide **17a** (126 mg, 0.206 mmol) was reduced with $NaBH_4$ (32 mg, 0.845 mmol) using a procedure similar to that described earlier to afford the title compound **17a** as yellow oil (75 mg, 57%): R_f = 0.54 [$CHCl_3$/MeOH (90:10)]; ^{1}H NMR ($CDCl_3$) δ 1.79−1.85 (m, 2H0, 2.04−2.12 (m, 4H), 2.43−2.45 (br s, 5H0, 2.54−2.57 (m, 2H), 3.43−3.57 (m, 10H), 4.47−4.55 (m, 4H), 7.03−7.05 (m, 1H); ^{13}C NMR ($CDCl_3$) δ 26.87, 29.44, 29.54, 30.25, 46.15, 51.47, 55.27, 57.69, 67.25, 67.46, 68.04, 68.14, 68.19, 68.28, 128.54, 129.63, 147.06, 151.09, 152.58, 162.61

Di(ethylene glycol)(3-methoxy-1,2,5-thiadiazol-4-yl) [3-(1-Methyl-1,2,5,6-tetrahydropyrid-3-yl)-1,2,5-thiadiazol-4-yl] Ether Hydrochloride (13a, CDD-0309A). The free base **12a** (141 mg, 0.352 mmol) was redissolved in a mixture of CH_3OH/$CHCl_3$ (10 mL, 5:5) and was cooled to 0 °C. Then, dry HCl gas was bubbled through the solution for 3 min, and the title compound **13a** was recrystallized from anhydrous acetone/ether to afford a white powder (97 mg, 88% yield): mp 130−131 °C; ^{1}H NMR ($CDCl_3$) δ 2.56 (s, 1H), 2.93 (s, 3H), 2.96 (s 1H), 3.20 (s, 1H), 3.53 (s, 1H), 3.75 (s, 1H), 3.90−3.94 (m, 4H), 4.07 (s, 1H), 4.45 (s, 1H), 4.56−4.58 (t, 2 H), 4.62 (m, 2H); ^{13}C NMR ($CDCl_3$) δ 22.78, 43.17, 49.88, 51.89, 57.56, 69.26, 69.39, 69.97, 70.19, 123.70, 127.37, 144.27, 151.61, 152.52, 162.32; ESI-MS m/z (free base) 400.3 [M + H$^+$]. Anal. ($C_{15}H_{21}N_5O_4S_2$·HCl) C, H, N.

Tri(ethylene glycol)(3-methoxy-1,2,5-thiadiazol-4-yl) [3-(1-Methyl-1,2,5,6-tetrahydropyrid-3-yl)-1,2,5-thiadiazol-4-yl] Ether Hydrochloride (13b, CDD-0311A). The free base **12b** (50 mg, 0.113 mmol) was recrystallized from anhydrous acetone/ethereal HCl solution at 0 °C to afford a pale yellow solid (46 mg, 75% yield): mp 84−85 °C; ^{1}H NMR ($CDCl_3$) δ 2.54 (m, 1H), 3.08 (m, 5H), 3.70 (s, 4H), 3.80 (m, 6H), 4.07 (s, 3H), 4.52 (m, 5H), 7.27 (s, 1H); ESI-MS m/z (free base) 444.3 [M + H$^+$], 466.2 [M + Na]. Anal. ($C_{17}H_{25}N_5O_5S_2$·HCl·1.5 H_2O·0.5$C_4H_{10}O$) C, H, N.

Penta(ethylene glycol)(3-methoxy-1,2,5-thiadiazol-4-yl) [3-(1-Methyl-1,2,5,6-tetrahydropyrid-3-yl)-1,2,5-thiadiazol-4-yl] Ether Hydrochloride (13d, CDD-0310A). The free base **12d** (91 mg, 0.171 mmol) was recrystallized from anhydrous acetone/ethereal HCl solution at 0 °C to afford a pale yellow semisolid (70 mg, 69% yield): ^{1}H NMR ($CDCl_3$) δ 2.55 (m, 1H), 2.93 (m, 3H), 2.99 (m, 1H), 3.22 (m, 1H), 3.52 (m, 1H), 3.62 (m, 12H), 3.67 (m, 1H), 3.84 (s, 4H), 4.07 (s, 3H), 4.46 (m, 1H), 4.53 (m, 2H), 4.57 (m, 2H), 7.27 (s, 1H); ESI-MS m/z (free base) 532.1 [M + H], 554.1 [M + Na]. Anal. ($C_{21}H_{33}N_5O_7S_2$·HCl·1.25 H_2O) C, H, N.

Tri(propylene glycol)(3-methoxy-1,2,5-thiadiazol-4-yl) [3-(1-Methyl-1,2,5,6-tetrahydropyrid-3-yl)-1,2,5-thiadiazol-4-yl] Ether Hydrochloride (18a, CDD-0314A). The free base **17a** (75 mg, 0.154 mmol) was recrystallized from anhydrous acetone/ethereal HCl solution at 0 °C to afford a pale yellow solid (60 mg, 73% yield): mp 62−64 °C; ^{1}H NMR ($CDCl_3$) δ 1.78−1.83 (m, 2H), 2.04−2.10 (m, 4H), 2.53−2.57 (br s, 1H), 2.93 (s, 3H), 2.98 (br s, 1H), 3.21 (br s, 1H), 3.46−3.49 (m, 4H), 3.52−3.55 (m, 5H), 3.73 (br s, 1H), 4.07 (s, 3H), 4.46 (t, 3H), 4.53 (t, 3H), 7.22 (br s, 1H); ^{13}C NMR ($CDCl_3$) δ 22.81, 29.44, 29.49, 30.24, 43.25, 49.93, 51.96, 57.74, 67.24, 67.39, 68.03, 68.19, 68.94, 123.96, 126.91, 144.10, 151.90, 152.58, 162.60; ESI-MS m/z (free base) 486.1 [M + H$^+$], 508 [M + Na]. Anal. ($C_{20}H_{31}N_5O_5S_2$·HCl·0.5H_2O) C, H, N.

Tetra(ethylene glycol)(3-methoxy-1,2,4-thiadiazol-5-yl) [3-(Pyrid-3-yl)-1,2,5-thiadiazol-4-yl] Ether (10e). A suspension of 60% NaH in mineral oil (128 mg, 3.20 mmol) was washed with anhydrous hexane and suspended in freshly distilled THF (30 mL). Then, **9c** (280 mg, 0.787 mmol) in THF (50 mL) was added to the above suspension and the reaction mixture was refluxed for 1 h. Compound **6** (275 mg, 1.82 mmol) in THF (40 mL) was added, and the reaction mixture was refluxed for 5 days. The mixture was evaporated under vacuum and quenched with ice water (50 mL). The aqueous solution was extracted twice with $CHCl_3$, and the combined organic extracts were dried over anhydrous Na_2SO_4 and concentrated to yield the crude compound. After silica gel chromatography with CH_2Cl_2/MeOH (10 mL:15 drops), **10e** was obtained as yellow oil (250 mg, 50%): R_f = 0.24 [CH_2Cl_2/MeOH (10:0.2)]; ^{1}H NMR (CDCl3) δ 3.63 (s, 4H), 3.65−3.66 (t, 2H), 3.69−3.71 (t, 2H), 3.80−3.82 (t, 2H), 3.91−3.93 (t, 2H), 3.97 (s, 3H), 4.57−4.59 (t, 2H), 4.65−4.68 (t, 2H), 7.36−7.39 (m, 1H), 8.41−8.44 (d, J = 8.4, 1H), 8.62−8.63 (dd, J = 1.6 and 4.8, 1H), 9.38 (s, 1H); ^{13}C NMR ($CDCl_3$) δ 56.33, 69.39, 70.45, 70.84, 70.94, 70.98, 73.08, 123.61, 127.78, 135.01, 145.30, 148.91, 150.36, 162.72, 166.29, 190.37, 194.80.

Tri(propylene glycol)(3-methoxy-1,2,4-thiadiazol-5-yl) [3-(Pyrid-3-yl)-1,2,5-thiadiazol-4-yl] Ether (15b). Compound **15b** was prepared from **14** (415 mg, 1.17 mmol), **6** (265 mg, 1.76 mmol), and NaH (90 mg, 2.25 mmol) using a procedure similar to that described earlier to afford the title compound **15b** as yellow oil (142 mg, 26%): R_f = 0.51 [$CHCl_3$/MeOH (95:5)]; ^{1}H NMR ($CDCl_3$) δ 1.78−1.85 (m, 2H), 2.02−2.08 (m, 2H), 2.12−2.18 (2H), 3.46−3.53 6H), 3.59−3.62 (t, 2H), 3.98 (s, 3H), 4.51−4.54 (t, 2H), 4.61−4.64 (t, 2H), 7.38−7.41 (m, 1H), 8.41 (d, J = 8.0 Hz, 1H), 8.64 (dd, J = 1.6 and 5.2 Hz, 1H), 9.38 (s, 1H); ^{13}C NMR ($CDCl_3$) δ 29.23, 29.50, 30.16, 56.29, 66.74, 67.35, 68.07, 68.75, 71.45, 123.62, 127.80, 134.90, 145.11, 148.75, 150.33, 162.87, 166.47, 190.45

Tetra(ethylene glycol)(3-methoxy-1,2,4-thiadiazol-5-yl) [3-(1-Methyl-1,2,5,6-tetrahydropyrid-3-yl)-1,2,5-thiadiazol-4-yl] Ether (12e). To a solution of **10e** (250 mg, 0.532 mmol) in acetone/$CHCl_3$ (10:2 mL) was added CH_3I (4 mL, 64 mmol), and the solution was stirred under nitrogen for 1 week at room temperature. The residual quaternary iodide **11e** was obtained by removing the solvents under reduced pressure to afford a pale yellow solid and was used immediately without further purification: R_f = 0.27 [CH_2Cl_2/MeOH (9:1)]; ^{1}H NMR ($CDCl_3$) 3.64−3.68 (m, 4H), 3.72−3.74 (m, 2H), 3.79 (s, 2H), 3.82−3.84 (m, 2H), 3.96−3.99 (m, 5H), 4.54−4.57 (m, 2H), 4.73−4.75 (m, 2H), 4.78 (s, 3H), 8.23−8.27 (m, 1H), 9.14 (d, J = 8.4 Hz, 1H), 9.52−9.54 (m, 2H). The pyridinium iodide **11e** (320 mg, 0.52 mmol) was dissolved in a mixture of CH_3OH (10 mL) and $CHCl_3$ (5 mL). The solution was cooled to 0−5 °C, and $NaBH_4$ (73 mg, 1.93 mmol) was added. After the mixture was stirred at 0−5 °C for 1 h, another 73 mg of $NaBH_4$ was added and then another 73 mg after 1 h. The reaction continued for 2 h. Ice water was added to the reaction mixture, which was then extracted twice with $CHCl_3$. The combined organic extract was washed with water, dried over anhydrous Na_2SO_4, and concentrated to give the crude compound. After the silica gel chromatography with CH_2Cl_2/MeOH (90:10), **12e** was obtained as a yellow oil (104 mg, 40%): R_f = 0.57 [CH_2Cl_2/MeOH (9:1)]; ^{1}H NMR ($CDCl_3$) δ 2.42−2.44 (m, 5H), 2.54−2.56 (t, 2H), 3.43 (m, 2H), 3.64−3.70 (m, 8H), 3.83−3.85 (t, 2H), 3.88−3.90 (t, 2H), 3.99 (s, 3H), 4.59−4.62 (m, 4H), 7.07−7.09 (m, 1H); ^{13}C NMR ($CDCl_3$) δ 26.70, 46.04, 51.40,

55.09, 56.36, 69.04, 69.47, 70.05, 70.86, 70.92, 70.97, 71.02, 73.10, 128.78, 129.19, 147.00, 162.41, 166.29, 190.38.

Tri(propylene glycol)(3-methoxy-1,2,4-thiadiazol-5-yl) [3-(1-Methyl-1,2,5,6-tetrahydropyrid-3-yl)-1,2,5-thiadiazol-4-yl] Ether (17b). Compound **16b** was prepared from **15b** (142 mg, 0.304 mmol) and CH_3I (2 mL, 24 mmol) using a procedure similar to that described earlier to provide the pyridinium iodide compound as a yellow oil: $R_f = 0.31$ [CH_2Cl_2/MeOH (90:10)]; ^{1}H NMR ($CDCl_3$) δ 1.74−1.85 (m, 2H), 2.04−2.10 (m, 2H), 2.18−2.25 (m, 2H), 3.46−3.64 (m, 8H), 3.99 (s, 3H), 4.50−4.56 (t, 2H), 4.68−4.74 (t, 2H), 4.82 (s, 3H), 8.26−8.33 (m, 1H), 9.14 (d, $J = 8.4$ Hz, 1H), 9.48 (s, 1H), 9.61 (d, $J = 6.0$ Hz, 1H). The pyridinium iodide **16b** (189 mg, 0.31 mmol) was reduced with $NaBH_4$ (50 mg, 1.31 mmol) using a procedure similar to that described earlier to afford the title compound **17b** as yellow oil (60 mg, 41%): $R_f = 0.43$ [CH_2Cl_2/MeOH (90:10)]; ^{1}H NMR ($CDCl_3$) δ 1.78−1.85 (m, 2H), 2.02−2.12 (m, 4H), 2.43−4.45 (br s, 5H), 2.54−2.57 (t, 2H), 3.43−3.58 (m, 10H), 3.99 (s, 3H), 4.52−4.55 (t, 4H), 7.03−7.04 (m, 1H); ^{13}C NMR ($CDCl_3$) δ 26.89, 29.29, 29.53, 30.21, 46.16, 51.47, 55.28, 56.32, 66.80, 67.47, 68.09, 68.13, 68.27, 71.48, 128.56, 129.63, 147.05, 162.61, 166.54, 190.52.

Tetra(ethylene glycol)(3-methoxy-1,2,4-thiadiazol-5-yl) [3-(1-Methyl-1,2,5,6-tetrahydropyrid-3-yl)-1,2,5-thiadiazol-4-yl] Ether Hydrochloride (13e, CDD-0313A). The free base **12e** (104 mg, 0.213 mmol) was redissolved in a mixture of $CH_3OH/CHCl_3$ (10 mL, 5:5) and was cooled to 0 °C. Then, dry HCl gas was bubbled through the solution for 3 min, and the title compound **13e** was recrystallized from anhydrous acetone/ether to afford a white semisolid (90 mg, 72% yield): ^{1}H NMR ($CDCl_3$) δ 2.54 (m, 1H), 2.92 (m, 3H), 2.98 (m, 1H), 3.17 (m, 1H), 3.52 (m, 1H), 3.59 (m, 10H), 3.71 (m, 3H), 3.82 (m, 1H), 3.85 (m, 2H), 3.96 (s, 1H), 4.44 (m, 1H), 4.57 (m, 3H), 7.26 (s, 1H); ^{13}C NMR ($CDCl_3$) δ 22.77, 43.05, 43.17, 49.91, 51.93, 55.55, 56.37, 69.32, 70.34, 70.81, 70.85, 70.92, 71.55, 73.11, 123.714, 127.40, 144.28, 162.39; ESI-MS *m*/*z* (free base) 488.1 [M + H$^+$]. Anal. ($C_{19}H_{29}N_5O_6S_2 \cdot HCl \cdot 1.25H_2O \cdot 0.5C_4H_{10}O$) C, H, N.

Tri(propylene glycol)(3-methoxy-1,2,4-thiadiazol-5-yl) [3-(1-Methyl-1,2,5,6-tetrahydropyrid-3-yl)-1,2,5-thiadiazol-4-yl] Ether Hydrochloride (18b, CDD-0316A). The free base **17b** (60 mg, 0.124 mmol) was recrystallized from anhydrous acetone/ethereal HCl solution at 0 °C to afford a pale yellow solid (40 mg, 53% yield): mp 77−80 °C; ^{1}H NMR ($CDCl_3$) δ 1.79−1.85 (m, 2H), 2.03−2.13 (m, 4H), 2.94−2.95 (d, 4H), 3.26 (br s, 1H), 3.46−3.57 (m, 10H), 3.75 (br s, 1H), 3.99 (s, 3H), 4.52−4.57 (m, 4H), 7.26 (s, 1H); ESI-MS *m*/*z* (free base) 486.3 [M + H$^+$]. Anal. ($C_{20}H_{31}N_5O_5S_2 \cdot 1.75HCl \cdot 0.5H_2O \cdot 0.75C_4H_{10}O$) C, H, N: calcd, 6.77; found, 6.30.

Pharmacology. Receptor Binding. Plasmids for muscarinic receptor subtypes were obtained either as a gift from Dr. Tom I. Bonner of the National Institutes of Health or from the UMR cDNA Resource Center (www.cdna.org). Membrane homogenates were prepared from transfected cells using established procedures.[33] All binding assays were conducted in a 1 mL mixture of binding buffer [25 mM sodium phosphate (pH 7.4) containing 5 mM magnesium chloride]. In ligand inhibition binding assays, 0.1 nM of [^{3}H]-(*R*)-QNB and 14 points for the test ligand (ranging from 0.01 nM to 3 mM) were used. The mixture was incubated for 2 h at room temperature. Total binding and nonspecific binding were determined in the absence and presence of 1000-fold excess of unlabeled (*R*)-QNB. Radioactivity was counted using a TopCount NXT system (Packard, Meriden, CT).

Phosphoinositide Hydrolysis Assays. To ascertain the functional properties of the novel compounds at the M_1, M_3, and M_5 mAChRs, assays of mAChR-mediated PI hydrolysis were conducted. The method is described as follows: A9 L cells stably expressing particular human muscarinic receptor subtypes were seeded into 96-well tissue culture plates for 24 h. Then 100 μL of inositol-free (IF) DMEM was added to each well, which was supplemented with 25 mM d-glucose, 4 mM L-glutamine, 0.6% BSA, and 10 μCi/mL [^{3}H]Ins. Cells were further incubated overnight. Test ligand dilutions were prepared in HBSS buffer supplemented with 10 mM LiCl and 20 mM HEPES. Incubation was initiated by addition of 100 μL of the proper concentration of test ligands (with the dilution buffer serving to measure basal levels) to each well in triplicate sets and carried out at 37 °C for 1 h. The incubation was stopped by rapid removal of all media. Then, 100 μL of ice-cold 50 mM formic acid was added to each well and allowed to sit at room temperature for 20 min. To 96 white solid plates was added 80 μL of YSi-SPA beads at 1 mg/80 μL water, followed by 20 μL of cell extract in formic acid. The plate was sealed with Topseal A, and the contents were mixed by shaking for 1 h in 4 °C room. After standing for 2 h, radioactivity in counts per minute (cpm) was determined using a TopCount NXT system. Activity is presented as the percentage activation above basal levels. Carbachol was utilized in each assay as a positive control for muscarinic receptor activation.

Cyclic AMP Assay. The M_2 and M_4 mAChRs signal preferentially through the cAMP pathway. Hence, ligands were investigated for their ability to inhibit forskolin-stimulated cAMP accumulation in cells expressing the human M_2 or M_4 mAChR.[34] The DiscovRx's HitHunter cAMP kit was used to test cyclic AMP levels. Carbachol was utilized in each assay as a positive control for muscarinic receptor activation.

Site-Directed Mutagenesis and Chimeric Receptor Studies. Site-directed mutagenesis and chimeric receptor studies were conducted using HM_1pcD and HM_5pcD plasmids using the Quikchange Site-Directed Mutagenesis Kit from Stratagene (La Jolla, CA). Mutations were confirmed by unique restriction digestion (if applicable) and dideoxynucleotide sequencing using the T7 Sequenase sequencing kits from Amersham Life Science Inc. (Arlington Heights, IL). A9 L cells were cotransfected with plasmids encoding mutant muscarinic receptors and pNEOβGal using the LIPOFECTIN reagent from Life Technologies (Gaithersburg, MD) or the calcium phosphate method.[35] The transfected A9 L cells were selected in DMEM (supplemented with 10% FBS, 4 mM L-glutamine, 50 unit/mL penicillin, and 50 μg/mL streptomycin) containing 800 μg/mL G418. Single cell colonies were transferred into 24-well plates for screening in both intact cell binding assays and functional assays.[32]

Data Analysis. Nonlinear least-squares curve-fitting was performed using DeltaGraph Version 4.5 for Macintosh and/or GraphPad Prism version 4 for PC. [^{3}H]-(*R*)-QNB saturation binding data were fit to a one-site binding model for determining B_{max} and K_d values. B_{max} is the maximal specific binding in femtomole per milligram of membrane protein; K_d (equilibrium dissociation constant) is the concentration of [^{3}H]-(*R*)-QNB at which 50% of the maximal specific binding sites were occupied by [^{3}H]-(*R*)-QNB.

Ligand inhibition binding data were fit to one-site and/or two-site competitive binding models. Statistical comparisons between one-site and multiple-site models were carried out using an *F* test with α set at the 0.05 level. K_i values (competitor-receptor dissociations equilibrium constant) were calculated from IC_{50} values (medium affinity values) according to the formula $K_i = IC_{50}/(1 + [D]/K_d)$, in which [D] and K_d denote the concentration and dissociation equilibrium constant of the radioligand, which were tested in the saturation binding assay. The pK_i values are the negative logarithm of the K_i. Statistical comparisons in receptor binding affinity and receptor activation were applied using analysis of variance by post-hoc Turkey−Kramer tests with α set at the 0.05 level. More complex models were chosen only if they provided a significantly better fit to the data from each experiment.

In PI hydrolysis assays, the stimulation levels of a series of concentrations were plotted versus the logarithm of the concentration. Data were fit to a one-site stimulation model as described in the equation $Y = (S_{max}X)/(EC_{50} + X)$, in which Y is the recorded stimulation at concentration X of the tested ligand, S_{max} is the maximal stimulation above basal level, and pEC_{50} is the negative logarithm of the concentration of ligand needed to elicit 50% of the maximal response (EC_{50}). In cAMP assays, cAMP levels of a series of concentrations were plotted versus the logarithm of the concentration. Data were fit to sigmoidal dose−response curve with a variable slope model as described in the following: $Y =$ bottom

$+$ (top $-$ bottom)/(1 $+$ $10^{((\log EC_{50} - X)\text{Hill slope})}$), in which Y is the recorded release at concentration X of the tested ligand, bottom is the baseline response, top is the maximum response, I_{max} is the maximal inhibition above control level for the given ligand, and pIC_{50} is the negative logarithm of the concentration that evokes a response halfway between baseline and maximum (EC_{50}).

A two-way (ligand $\times$ receptor) analysis of variance (ANOVA) followed by Bonferroni post-test was performed to analyze differences in functional activities and receptor binding affinities. P values were set at 0.05 for determining significant differences.

Behavioral Studies. Animals and Equipment. Young, male Sprague−Dawley rats weighing 250−300 g were used in the prepulse inhibition studies using methods adapted from Stanhope et al.[22] Rats were tested in startle chambers (SR-LAB, San Diego Instruments, San Diego, CA), using piezoelectric accelerometers to record movement of the rat in response to startle stimuli. A loudspeaker was used to deliver background white noise and the prepulse and startle stimuli, all controlled by SR-LAB software. Responses were digitized and recorded to measure the peak startle amplitude during the first 200 ms following the pulse stimulus. Sound levels and accelerometer responses were calibrated prior to use.

Prepulse Inhibition Testing. Rats were habituated to the startle apparatus 1 day prior to testing. After 5 min of background noise (70 dB) to initiate the habituation session, animals were exposed to different auditory stimuli. Animals received 10 consecutive startle stimulus trials (120 dB) that last 100 ms. Then animals received 15 of each of two trial types: (i) startle stimulus (120 dB, 100 ms) and (ii) startle stimulus preceded 200 ms by a 20-ms prepulse 12 dB above background noise. The trial types were interspersed throughout the testing period. The intertrial interval varied between 30 and 60 s, and sessions lasted approximately 25 min. For testing, animals were habituated for 5 min with background noise before exposure to different auditory stimuli. During the session, rats received 15 each of two trial types: (i) startle stimulus (120 dB, 100 ms) and (ii) startle stimulus preceded 200 ms by prepulses of 12 dB above background noise. Each prepulse lasted 20 ms. The two trial types were given pseudorandomly throughout the testing period. The intertrial interval varied between 30 and 60 s and sessions lasted approximately 25 min. A null stimulus (same as background) also was included. Up to two animals were tested at a single time in separate chambers.

Drugs. Drugs were prepared in distilled water or physiological saline and administered sc at a dose volume of 1 mL/kg. Twelve animals were tested for each treatment group. When tested alone, all drugs were administered 25 min prior to testing. When tested for the ability to block the effects of apomorphine, drugs were administered 25 min prior to testing, while apomorphine was administered 5 min before testing. Control animals were given the appropriate vehicle at the appropriate time point. The dose for apomorphine was 1.0 mg/kg, while the dose tested for haloperidol, clozapine, and *N*-desmethylclozapine was 1.0 mg/kg. Muscarinic agonists were tested in a dose range from 0.1 to 3 mg/kg.

Analyses. Apomorphine increases the mean startle amplitude and impairs the percentage of prepulse inhibition [100 − (startle amplitude on prepulse − pulse trials/startle amplitude on pulse alone trials) × 100]. Compounds with antipsychotic activity should not affect the percentage of prepulse inhibition when given alone but should reverse the effects of apomorphine.[21,36] Analysis of variance was used to compare the effects of compounds on prepulse inhibition in the presence or absence of apomorphine.

Molecular Modeling. Molecular dynamics simulations, using the Sybyl 7.1 software,[37] were performed for bifunctional ligands in the gas phase, in aqueous solution, and in the hypothesized binding pocket of the muscarinic receptor subtypes. Atomic charges for the ligand molecules and the receptor protein were accepted from the MMFF94 and the AMBER sets of Sybyl, respectively. In all calculations the Tripos force field was utilized. Gas-phase simulations that were 130 ps long with 1 fs time step were performed at $T = 310$ K, applying a nonbonded cutoff of 20 Å. The starting structures represented all-trans conformations along the spacer with the exception of a gauche OCCO moiety nearly at the mid of the molecules. The large nonbonded cutoff allowed consideration of the interactions for the end groups, resulting in spacer folding throughout the simulations.

In-solution MD simulations started from the last gas-phase conformations. Each solute was placed in a pre-equilibrated box of about 1050 TIP3P water molecules. Periodic boundary conditions were applied in NpT simulations at $T = 310$ and $p = 1$ atm. One or two chloride counterions were considered for neutralization, and 3 Na^+···Cl^- ion pairs were added to the system to mimic the isotonic saline concentration. For keeping the calculations tractable at 2 fs time step, a nonbonded cutoff of 8 Å and the SHAKE restrictions for single bonds were applied. With these simulation parameters 450 ps long equilibration phases were followed by 300 ps long production phases. Different atom···atom distance trajectories were calculated for characterizing the solute structures.

Binding modes for compounds **1**, **2c**, and **13e** were studied within the wild-type (WT) muscarinic-1 receptor and in the o2, o3, and o2+o3 chimeric receptors. For the WT receptor, we used our previous model[25] based on the experimental rhodopsin structure.[38] The chimeric receptors were developed by modifying the corresponding side chains on the basis of the primary structure of the M_5 subtype of the WT muscarinic receptor. The calculations were carried out by implicit consideration of the solvent effect through a distance-dependent dielectric constant with the formula $\epsilon = 4r$. The protonated tetrahydropyrimidene sites of the ligands were arranged in the hypothesized acetylcholine binding site so that the formation of an N−H···O hydrogen bond with the carboxylate group of the Asp105 residue was feasible. The other cationic or polar neutral site was located in the region between the o2 and o3 loops. Two series of 50-ps simulations followed by energy minimizations were carried out consecutively in each case, using 1-fs time-step without SHAKE restrictions and applying nonbonded cutoff of 8 Å. The temperature was targeted at 310 K, and a strong coupling to a thermal-bath was mimicked by a coupling parameter of 0.1 ps. The calculations were continued for 100 ps and applying a nonbonded cutoff of 20 Å. The large cutoff facilitated consideration of the interaction of the remote polar sites of the bound ligands. The final results (Table 4) were obtained from 400-ps calculations with applying the still large 14 Å nonbonded cutoff.

Acknowledgment. We thank Ms. Karen Papadakis for her secretarial assistance. The work was supported by NIH grants NS 31173 and NS 35127 and by Cognitive Pharmaceuticals Ltd.

Supporting Information Available: Results from elemental analysis. This material is available free of charge via the Internet at http://pubs.acs.org.

References

(1) Baumeister, A.; Francis, J. Historical development of the dopamine hypothesis of schizophrenia. *J. Hist. Neurol.* **2002**, *11* (3), 265−277.
(2) Kelleher, J. P.; Centorrino, F.; Albert, M. J.; Baldessarini, R. J. Advances in atypical antipsychotics for the treatment of schizophrenia: New formulations and new agents. *CNS Drugs* **2002**, *16* (4), 249.
(3) Friedman, J. I. Cholinergic targets for cognitive enhancement in schizophrenia: Focus on cholinesterase inhibitors and muscarinic agonists. *Psychopharmacology* **2004**, *172*, 45−53.
(4) Hyman, S. E.; Fenton, W. S. What are the right targets for psychopharmacology? *Science* **2003**, *299*, 350−351.
(5) Friedman, J. I.; Temporini, H.; Davis, K. L. Pharmacologic strategies for augmenting cognitive performance in schizophrenia. *Biol. Psychiatry* **1999**, *45*, 1−16.
(6) Shannon, H. E.; Rasmussen, K.; Bymaster, F. P.; Hart, J. C.; Peters, S. C.; Swedberg, M. D.; Jeppesen, L.; Sheardown, M. J.; Sauerberg, P.; Fink-Jensen, A. Xanomeline, an M(1)/M(4) preferring muscarinic cholinergic receptor agonist, produces antipsychotic-like activity in rats and mice. *Schizophr. Res.* **2000**, 249.
(7) Bymaster, F.; Felder, C.; Tzavara, E.; Nomikos, G.; Calligaro, D.; McKinzie, D. Muscarinic mechanisms of antipsychotic atypicality. *Prog. Neuro-Psychopharmacol. Biol. Psychiatry* **2003**, *27*, 1125−1143.

(8) Bodick, N. C.; Offen, W. W.; Shannon, H. E.; Satterwhite, J.; Lucas, R.; van Lier, R.; Paul, S. M. The selective muscarinic agonist xanomeline improves both the cognitive deficits and behavioral symptoms of Alzheimer's disease. *Alzheimer Dis. Assoc. Disord.* **1997**, *11* (suppl 4), S16−22.
(9) Bodick, N. C.; Offen, W. W.; Levey, A. I.; Cutler, N. R.; Gauthier, S. G.; Satlin, A.; Shannon, H. E.; Tollefson, G. D.; Rasmussen, F. P.; Bymaster, F.; Hurley, D. J.; Potter, W. Z.; Paul, S. M. Effects of xanomeline, a selective muscarinic receptor agonist, on cognitive function and behavioral symptoms in Alzheimer disease. *Arch. Neurol.* **1997**, *54* (4), 465−473.
(10) Rasmussen, T.; Fink-Jensen, A.; Sauerberg, P.; Swedberg, M. D.; Thomsen, C.; Sheardown, M. J.; Jeppesen, L.; Calligaro, D. O.; DeLapp, N. W.; Whitesitt, C.; Ward, J. S.; Shannon, H. E.; Bymaster, F. P. The muscarinic receptor agonist BuTAC, a novel potential antipsychotic, does not impair learning and memory in mouse passive avoidance. *Schizophr. Res.* **2001**, *49*, 193−201.
(11) Jones, C. K.; Shannon, H. E. Effects of scopolamine in comparison with apomorphine and phencyclidine on prepulse inhibition in rats. *Eur. J. Pharmacol.* **2000**, *391*, 105−112.
(12) Jones, C. K.; Shannon, H. E. Muscarinic cholinergic modulation of prepulse inhibition of the acoustic startle reflex. *J. Pharmacol. Exp. Ther.* **2000**, *294*, 1017−1023.
(13) Felder, C. C.; Porter, A. C.; Skillman, T. L.; Zhang, L.; Bymaster, F. P.; Nathanson, N. M.; Hamilton, S. E.; Gomeza, J.; Wess, J.; McKinzie, D. L. Elucidating the role of muscarinic receptors in psychosis. *Life Sci.* **2001**, *68*, 2605−2613.
(14) Levey, A. I. Muscarinic acetylcholine receptor expression in memory circuits: Implications for treatment of Alzheimer's disease. *Proc. Natl. Acad. Sci. U.S.A.* **1996**, *93* (24), 13541−13456.
(15) Dean, B. M1 receptor agonism, a possible treatment for cognitive deficits in schizophrenia. *Neuropsychopharmacology* **2004**, *29* (8), 1583−1584.
(16) Anagnostaras, S. G.; Murphy, G. G.; Hamilton, S. E.; Mitchell, S. L.; Rahnama, N. P. et al. Selective cognitive dysfunction in acetylcholine M1 muscarinic receptor mutant mice. *Nat. Neurosci.* **2003**, *6*, 51−58.
(17) Seeger, T.; Fedorova, I.; Zheng, F.; Miyakawa, T.; Koustova, E. et al. M2 muscarinic acetylcholine receptor knock-out mice show deficits in behavioral flexibility, working memory, and hippocampal plasticity. *J. Neurosci.* **2004**, *24*, 10117−10127.
(18) Tzavara, E.; Bymaster, F. P.; Felder, C. C.; Wade, M.; Gomeza, J.;Wess, J.; McKinzie, D. L.; Nomikos, G. G. Dysregulated hippocampal acetylcholine neurotransmission and impaired cognition in M2, M4 and M2/M4 muscarinic receptor knockout mice. *Mol. Psychiatry* **2003**, *8*, 673−679.
(19) Zhang, W.; Yamada, M.; Gomeza, J.; Basile, A. S.; Wess, J. Multiple muscarinic acetylcholine receptor subtypes modulate striatal dopamine release, as studied with M1−M5 muscarinic receptor knock-out mice. *Neuroscience* **2002**, *22* (15), 6347−6352.
(20) Tzavara, E.; Bymaster, F.; Davis, R.; Wade, M.; Perry, K.; Wess, J.; McKinzie, D.; Felder, C.; Nomikos, G. J. M4 muscarinic receptors regulate the dynamics of cholinergic and dopaminergic neurotransmission: Relevance to the pathophysiology and treatment of related central nervous system pathologies. *FASEB* **2004**, *18* (12), 1410−1412.
(21) Geyer, M. A.; Krebs-Thomson, K.; Braff, D. L.; Swerdlow, N. R. Pharmacological studies of prepulse inhibition models of sensorimotor gating deficits in schizophrenia: A decade in review. *Psychopharmacology* (*Berlin*) **2001**, *156*, 117−154.
(22) Stanhope, K. J.; Mirza, N. R.; Bickerdike, M. J.; Bright, J. L.; Harrington, N. R.; Hesselink, M. B.; Kennett, G. A.; Lightowler, S.; Sheardown, M. J.; Syed, R.; Upton, R. L.; Wadsworth, G.; Weiss, S. M.; Wyatt, A. The muscarinic receptor agonist xanomeline has an antipsychotic-like profile in the rat. *J. Pharmacol. Exp. Ther.* **2001**, 782−792.
(23) Li, Z.; Kim, C. H.; Ichikawa, J.; Meltzer, H. Y. Effect of repeated administration of phencyclidine on spatial performance in an eight-arm radial maze with delay in rats and mice. *Pharmacol. Biochem. Behav.* **2003**, 335−340.
(24) Goldman-Rakic, P. S.; Selemon, L. D. Functional and anatomical aspects of prefrontal pathology in schizophrenia. *Schizophr. Bull.* **1997**, *23*, 437−458.
(25) Rajeswaran, W. G.; Cao, Y.; Huang, X.-P.; Wroblewski, M. E.; Colclough, T.; et al. Design, synthesis, and biological characterization of bivalent 1-methyl-1,2,5,6-tetrahydropyridyl-1,2,5-thiadiazole derivatives as selective muscarinic agonists. *J. Med. Chem.* **2001**, *44*, 4563−4576.
(26) Cao, Y.; Zhang, M.; Wu, C.; Lee, S.; Wroblewski, E.; Whipple, T.; Nagy, P.; Novak, K. T.; Balazs, A.; Toros, S.; Messer, W. S., Jr. Synthesis and biological characterization of 1-methyl-1,2,5,6-tetrahydropyridyl-1,2,5-thiadiazole derivatives as muscarinic agonists for the treatment of neurological disorders. *J. Med. Chem.* **2003**, *46*, 4273−4286.
(27) Sauerberg, P.; Olesen, P. H.; Nielsen, S.; Treppendahl, S.; Sheardown, M. J.; Honore, T.; Mitch, C. H.; Ward, J. S.; Pike, A. J.; Bymaster, F. P. Novel functional M1 selective muscarinic agonists. Synthesis and structure−activity relationships of 3-(1,2,5-thiadiazolyl)-1,2,5,6-tetrahydro-1-methylpyridines. *J. Med. Chem.* **1992**, 2274−2283.
(28) Karimian, K. T.; Tam, F.; Leung-Toung, R. C. S. H.; Li, W.; Bryson, S. P.; Wodzinska, J. M. Preparation of thiadiazole amino acid derivatives as inhibitors of cysteine activity dependent enzymes. U.S. Patent 6,162,791 2002, pp 1−35.
(29) Gerber, S. A.; Tureek, F.; Gelb, M. H. Design and synthesis of substrate and internal standard conjugates for profiling enzyme activity in the Sanfilippo syndrome by affinity chromatography/electrospray ionization mass spectrometry. *Bioconjugate Chem.* **2001**, *12*, 603−615.
(30) Golla, R.; Seethala, R. A homogeneous enzyme fragment complementation cyclic AMP screen for GPCR agonists. *J. Biomol. Scr.* **2002**, *7*, 515−525.
(31) Huang, X. P.; Nagy, P. I.; Williams, F. E.; Peseckis, S. M.; Messer, W. S., Jr. Roles of threonine 192 and asparagine 382 in agonist and antagonist interactions with M1 muscarinic receptors. *Br. J. Pharmacol.* **1999**, *126*, 735−745.
(32) Huang, X. P.; Williams, F. E.; Peseckis, S. M.; Messer, W. S., Jr. Pharmacological characterization of human m1 muscarinic acetylcholine receptors with double mutations at the junction of TM VI and the third extracellular domain. *J. Pharmacol. Exp. Ther.* **1998**, *286*, 1129−1139.
(33) Huang, X. P.; Williams, F. E.; Peseckis, S. M.; Messer, W. S., Jr. Differential modulation of agonist potency and receptor coupling by mutations of Ser388Tyr and Thr389Pro at the junction of transmembrane domain VI and the third extracellular loop of human M(1) muscarinic acetylcholine receptors. *Mol. Pharmacol.* **1999**, *56*, 775−783.
(34) Harper, J. F.; Booker, G. Femtomole sensitive radioimmunoassay for cyclic AMP and cyclic GMP after 20 acetylation by acetic anhydride in aqueous solution. *J. Cycl. Nucleotide Res.* **1975**, *1*, 207−218.
(35) Chen, C.; Okayama, H. High-efficiency transformation of mammalian cells by plasmid DNA. *Mol. Cell Biol.* **1987**, *7*, 2745−2752.
(36) Kumari, V.; Sharma, T. Effects of typical and atypical antipsychotics on prepulse inhibition in schizophrenia: A critical evaluation of current evidence and directions for future research. *Psychopharmacology (Berlin)* **2002**, *162*, 97−101.
(37) Version 7.1; Tripos Inc.: St. Louis, Mo. *Sybyl* 2005.
(38) Palczewski, K.; Hori, T.; Behnke, C. A.; Motoshima, H.; Fox, B. A.; Le Trong, I.; Teller, D. C.; Okada, T.; Stenkemp, R. E.; Yamamoto, M.; Miyano, M. Crystal Structure of rhodopsin: A G-protein receptor. *Science* **2000**, *289*, 739−745.

JM0606995